Exploring the Influence of Progranulin on Vascular Contractility and Mitochondrial Homeostasis

by

Shubhnita Singh

M.D., University of Mauritius, 2014

Submitted to the Graduate Faculty of the

Department of Human Genetics

School of Public Health in partial fulfillment

of the requirements for the degree of

Doctor of Philosophy

University of Pittsburgh

2023

UNIVERSITY OF PITTSBURGH

SCHOOL OF PUBLIC HEALTH

This dissertation was presented

by

Shubhnita Singh

It was defended on

November 9, 2023

and approved by

Zsolt Urban, PhD, Associate Professor of Human Genetics, School of Public Health, University of Pittsburgh

Quasar Padiath, MBBS, PhD, Associate Professor of Human Genetics, School of Public Health, University of Pittsburgh

Eric S. Goetzman, PhD, Associate Professor of Human Genetics, School of Public Health, University of Pittsburgh

Delphine Anne Henriette Gomez, PhD, Assistant Professor of Medicine, School of Medicine, University of Pittsburgh

Thiago Bruder do Nascimento, PhD, **Dissertation Director**
Assistant Professor of Pediatrics, School of Medicine, University of Pittsburgh

Exploring the Influence of Progranulin on Vascular Contractility and Mitochondrial Homeostasis

Shubhnita Singh, PhD

University of Pittsburgh, 2023

Cardiovascular diseases (CVDs) encompass a spectrum of conditions impacting the heart and blood vessels, attributing to around 19.1 million global deaths in 2020. These diseases can be congenital, acquired, or have a hereditary basis. Vascular smooth muscle cells (VSMCs) are crucial in maintaining vessel structure, diameter regulation, and vascular calcification—central processes in CVDs. Progranulin (PGRN), a glycoprotein, plays diverse roles in various tissues and cell types, involving embryogenesis, inflammation, wound healing, neurodegeneration, and lysosomal function. Mutations in the granulin (GRN) gene causing PGRN protein insufficiency lead to neurodegeneration. Our research reveals the significance of PGRN in protecting against CVDs.

Analyzing aorta from PGRN-deficient mice, we discovered reduced aortic contractility, unveiling a new facet of PGRN's function. RNA sequencing showed suppressed oxidative phosphorylation (OXPHOS) in aortae from PGRN knockout mice, notably downregulating genes related to complex I activity in the electron transport chain pathways.

PGRN's functions span cell growth, embryogenesis, anti-inflammatory responses, and wound healing. We propose studying the molecular mechanisms behind mutant PGRN, potentially driving cardiovascular defects. Primary VSMCs from PGRN knockout mice exhibited perturbed contraction, reduced oxygen consumption rate (OCR), and impaired mitophagy, paralleled by lower ATP levels and increased mitochondrial oxidative stress due to PGRN deficiency.

Increasing PGRN expression through a viral vector significantly improved vascular contractility, OCR, mitochondrial complex I activity, and reduced oxidative stress. PGRN deficiency disrupted lysosomal function within VSMCs, affecting mitophagy. In a model with chronic Angiotensin II treatment, PGRN-deficient mice displayed unresponsiveness in hypercontractility and increased collagen deposition.

Our research underscores PGRN's crucial role in maintaining vascular contractility by regulating mitochondrial function. With the need for novel CVD therapies, these findings are significant. PGRN's influence on mitochondrial complex I quality, mitochondria recycling, and redox signaling pathways suggest its potential as a therapeutic target for CVDs, positioning PGRN as a promising alternative in treatment strategies.

Table of Contents

List of Tables

List of Figures

Preface

In the course of my four-year journey through the Ph.D. program, I've experienced moments of intrigue, joy, and also faced significant challenges. As I begin this dissertation, I feel compelled to formally acknowledge the individuals who have supported me, nurtured my growth, and kept me grounded throughout this transformative period. Words may fall short of conveying the depth of gratitude I hold for these individuals in my heart. Foremost, I wish to express my profound appreciation for my mentor, Dr. Thiago Bruder do Nascimento. I liken every student to a blank canvas and shaping that canvas into a masterpiece demands exceptional skill, boundless patience, and unwavering dedication. Dr. Bruder's exceptional guidance, scientific brilliance, and steadfast support have been instrumental in my transformation from a physician into a physician-scientist. Our in-depth meetings have ignited my passion for science, encouraged me to learn from my mistakes, and instilled a whole-hearted commitment to each experiment. Whether my experiments yielded disappointing results or exciting breakthroughs, Dr. Bruder's support remained steadfast. He has been an exceptional role model, and I consider myself immensely fortunate to have been guided by him. Reflecting on my journey, I'm reminded of a quote from a favorite book of mine: “What is more important—the journey or the destination? The company”. Throughout my four years, I've had the privilege of being in the remarkable company of our lab manager, Dr. Ariane Bruder do Nascimento. I extend my heartfelt gratitude to her for her kindness, unwavering readiness to answer my questions, and her extraordinary patience with my numerous mistakes. Dr. Nascimento has been both my laboratory mentor and a dear friend, a bond I will cherish for a lifetime.

I would like to express my heartfelt appreciation to the entire Bruder laboratory, affectionately known as the 'Brudities.' They have been my unwavering support system throughout these years. My deepest gratitude goes to Dr. Rafael Menezes da Costa for his kindness and consistent assistance, always being my go-to person. I extend my thanks to our visiting students, Juliano Vilela, Wanessa Awata, and Gabriela Barbosa, as well as our summer students, Anita Bargaje, Rohit Guru, Mia DelVecchio, Nicole Kondrich, and Antonio Hernandez. The unforgettable moments we shared will remain etched in my memory forever. The laboratory's nurturing environment has played a pivotal role in my growth as a scientist and has been a source of solace, making every moment of work a joyous experience. I'd also like to extend my heartfelt gratitude to Dr. Debora M. Cerqueira, Dr. Cristina Espinosa Diez, Dr. Katherine Maringer, and Dr. Merlin Airik. They are not just brilliant scientists but also incredible friends who have supported me in navigating both my Ph.D. journey and life in general. A special shout-out goes to my friends Dr. Jia QiCheng Zhang, Elynna Youm, Sierra McKinzie, Wafaa Albalawy, Keaton Solo, and Anokhi Kashiparekh, who have been by my side since the very beginning of graduate school. I'm deeply thankful to the members of my thesis committee: Dr. Zsolt Urban, Dr. Quasar Padiath, Dr. Eric S. Goetzman, and Dr. Delphine Gomez. I would also like to express my appreciation to the members of the Goetzman lab, especially Dr. Sivakama Bharathi. Her technical guidance and valuable scientific insights have been instrumental in my research journey. I'm indebted to all the neighboring labs in Rangos, particularly the Sims Lucas, Ho, and Lucas-McAllister labs, for fostering an inspiring, collaborative, and educational laboratory environment. I would also like to recognize Dr. Udai Pandey for his invaluable guidance throughout my Ph.D. journey and for providing me the opportunity to rotate in his lab, especially during the challenging times of the COVID-19 pandemic. I am deeply thankful to Dr. Jerry Vockley and Dr. Dwi

Kemaladewi for their support during my fellowship application process. I am profoundly grateful to the Graduate School of Public Health and the Department of Human Genetics for granting me the opportunity to pursue my Ph.D. I want to acknowledge Dr. Candace Kammerer, whose guidance I immensely appreciated during the pandemic, and Dr. Beth Roman for her guidance and mentorship.

No words can fully express the profound depth of gratitude I hold for my parents, Ramayan Pratap Singh, and Usha Singh. Their unwavering love, support, and encouragement have been my pillars of strength throughout this journey. Their prayers, motivational words, and frequent video calls have bridged the physical distance and kept us emotionally connected. I am equally grateful to my five additional parents, my four elder sisters, and my brother—Jyotsna Singh, Anamika Singh, Santwana Singh, Sonal Singh, and Naveen Pratap Singh. Their boundless love, constant care, and unwavering support have been my rock. I extend my heartfelt thanks to my brothers-in-law and sister-in-law, as well as my beloved nieces and nephews. Having in-laws who stand by your side and support your dreams is a true blessing, I want to express my deepest appreciation to the other half of my family—S.D.Vijayaraghavan and Meenakshi Vijayaraghavan. Your love and support have meant the world to me.

Last, but certainly not least, I wish to express my deep gratitude to my husband, Dr. Rajan Vijayaraghavan. From day one, he has been my constant cheerleader, urging me to reach higher in life and always believing in me. These past four years have presented their fair share of challenges, particularly in the midst of the uncertainty brought about by the pandemic and living on separate continents. Your words of encouragement whispered in moments of doubt have provided me with the strength to overcome obstacles and persevere. Rajan has consistently filled my life with love and joy. His steadfast determination and enthusiasm have not only increased my

patience and empathy but have also broadened my overall outlook on life. As I continue to pursue my dreams, I want you to know that your presence in my life is the most profound blessing. Your love has been my anchor, and your steadfast support has been my wings. Thank you for being my partner, my confidant, and my most ardent supporter.

1.0 Introduction

1.1 Cardiovascular Diseases

Cardiovascular diseases (CVDs) represent the leading global cause of mortality, accounting for approximately 17.9 million deaths each year[1]. In the United States alone, CVDs result in a fatality every 33 seconds, with a substantial proportion occurring prematurely in individuals under 70 years of age[2]. CVDs encompasses a spectrum of heart and blood vessel disorders, including but not limited to coronary heart disease, cerebrovascular disease, and rheumatic heart disease. In blood vessels, vascular smooth muscle cells (VSMCs) residing in the medial layer play an indispensable role in upholding vascular function. Under normal physiological conditions, VSMCs are responsible for finely regulating vascular tone and diameter[3]. They possess the ability to respond to biomechanical stresses stemming from hemodynamic fluctuations and significantly contribute to determining the stiffness of the vascular wall[4].

However, when subjected to various stimuli such as endothelial injury, growth factors, and metabolic irregularities, VSMCs can undergo a transition from a contractile to a more proliferative and synthetic phenotype[5]. This phenotypic shift is notably observed in pathological contexts associated with a wide spectrum of CVDs, including atherosclerosis[6], stroke[6], and myocardial infarction[7]. Given the substantial impact of CVDs, there is an urgent imperative within the healthcare sector to prioritize the development of innovative therapeutic strategies. These approaches should aim either to restore VSMC contractility or prevent the phenotypic switching

of VSMCs, addressing a critical aspect of CVDs management. Our research has unveiled a novel regulator of vascular contractility, known as Progranulin (PGRN).

1.2 Progranulin: Structure and Regulation

PGRN serves as a versatile growth factor and plays a crucial role as an anti-inflammatory molecule. Its significance extends to the maintenance and regulation of homeostatic processes in normal tissue development, regeneration, host defense responses, and cell proliferation. PGRN, alternatively referred to as acrogranin, GP88, PC-derived growth factor, epithelin precursor and proepithelin, is the product of the GRN gene located on human chromosome 17q21[8-10]. Full length PGRN contains 7½ tandem, non-identical repeats of a cysteine-rich motif (CX5-6CX5CCX8CCX6C CXDX2HCCPX4CX5-6C, X: any amino acid) separated by 7 linker regions (P1-P7) in the order P-G-F-B-A-C-D-E, where A-G are full repeats, and P is the 1/2 motif[9, 11, 12].PGRN is a protein with a strong degree of conservation, found in a wide range of species such as zebrafish, *C. elegans*, rodents and humans[13-15]. PGRN undergoes proteolytic cleavage to form 6 KDa peptides known as granulins (A-G). Each granulin domain typically harbors 12 cysteine residues, resulting in the formation of 6 disulfide bonds, thereby creating a tightly packed β-sheet structure[15-17]. The cleavage of PGRN into granulins can be facilitated by various proteases, including matrix metallopeptidases[18, 19], disintegrin, elastases, cathepsins[20, 21], and neutrophil serine proteinase 3[22]. It is important to highlight that PGRN can manifest its effects either as a complete protein or via its granulin components. Notably, granulins play a distinct role in mitigating the effects of the complete protein, especially in processes like inflammation and neuroprotection[23, 24]. Another anti-inflammatory secretory protein that

frequently coexists with PGRN is Secretory leukocyte protease inhibitor (SLPI)[25]. SLPI exerts its protective function by inhibiting serine proteases and binding within sequences situated between granulin modules. This action forms a protective barrier around the full-length PGRN, effectively shielding it from proteolysis by elastase and various other proteases[10].

1.3 Progranulin: Synthesis and Transport

PGRN is distributed among diverse cell types throughout the body, including but not limited to epithelial cells, hematopoietic cells, neurons, and various vascular cells such as endothelial cells and VSMCs[9, 26-30].PGRN synthesis commences within the endoplasmic reticulum, where it is subject to an array of post-translational modifications[31-33].Following its synthesis, PGRN traverses the secretory pathway, and it may either be sequestered intracellularly within dense-core vesicles or exocytosed. In the extracellular milieu, PGRN assumes a dual role, functioning as an autocrine and paracrine growth factor. This functionality enables the transmission of signaling cues through a diverse array of receptors, such as EphrinA2 (EphA2)[34], Notch[35], and the tumor necrosis factor receptor (TNFR), acting as an antagonist[36].In the extracellular space, PGRN is also capable of binding to sortilin-1, a membrane protein that induces PGRN endocytosis, directing PGRN through the endosome and multivesicular bodies (MVBs) to ultimately reach the lysosome for subsequent cleavage and degradation[37]. Within the intracellular environment, PGRN predominantly localizes to endo-lysosomes, where it operates as an autocrine growth factor[38, 39]. Moreover, intracellular PGRN exhibits the capacity to modulate the functions of both cellular and viral transcription factors,

thereby influencing various cellular processes such as inflammatory responses, cell migration, and proliferation[40, 41].

1.4 Progranulin: Impact on Disease Pathophysiology

PGRN and Neurodegeneration

PGRN is widely explored in the field of neuroscience due to its significant associations with various neurodegenerative disorders. Reduced PGRN levels have been linked to conditions like Parkinson's disease (PD), Alzheimer's disease (AD), amyotrophic lateral sclerosis (ALS), limbic-predominant age-related transactivation response DNA-binding protein 43 (TDP-43) encephalopathy, and autism[42, 43]. On the other end of the spectrum, individuals with homozygous GRN mutations experience the complete loss of PGRN, leading to neuronal ceroid lipofuscinosis (NCL), a lysosomal storage disease typically affecting children[44, 45]. NCL is characterized by intracellular accumulation of lipofuscin, pigmented protein and lipid residue, as a consequence of impaired lysosomal proteolysis. In contrast, heterozygous mutations in the GRN gene result in PGRN haploinsufficiency, contributing to the development of frontotemporal lobar dementia (FTLD)[46]. FTLD is one of the most prevalent forms of dementia, typically occurring before the age of 65 and second only to Alzheimer's disease (AD) in terms of frequency[47].

Expanding Horizons: PGRN's Diverse Roles Beyond Neurodegenerative Diseases

While PGRN has been extensively explored in the center nervous system (CNS), recent findings indicate its vital role in immune response modulation, inflammatory resolution, and the influence on metabolic diseases [48, 49]. The research which initially proposed the anti-inflammatory function of PGRN demonstrated its capacity to inhibit the activation of neutrophils

induced by TNF-α[36]. Additionally, recombinant PGRN (rPGRN) ameliorated the impaired wound-healing observed in mice deficient in SLPI[10]. Conversely, PGRN knockout (KO) mice have an exacerbated inflammatory phenotype, coinciding with diminished host defense against *Listeria monocytogenes* infection[50]. Moreover, upon exposure to lipopolysaccharide (LPS) stimulation, bone marrow-derived macrophages (BMDMs) lacking PGRN exhibited elevated production of proinflammatory cytokines, including MCP-1, IL-12p40, IL-6, and TNF-α, while concurrently displaying reduced IL-10 levels compared to their wild-type (WT) counterparts[50]. The underlying mechanism responsible for this heightened cytokine response in PGRN-deficient macrophages was ascribed to the attenuation of IL-10 production. This association between PGRN and IL-10 production was further substantiated by two subsequent *in vivo* studies, both of which documented elevated levels of mouse serum IL-10 subsequent to the administration of rPGRN or the introduction of the Grn transgene[36, 51].

PGRN demonstrates protective and therapeutic effects in various joint diseases, including collagen and antibody-induced arthritis, spontaneous arthritis, and intervertebral-disc (ID) degeneration[52, 53]. These properties were substantiated in a mouse model of collagen-induced arthritis (CIA), which closely mirrors both the immunological and pathological features of human rheumatoid arthritis. Significantly, PGRN deficient mice display more pronounced inflammatory arthritis and increased damage in bone and joint tissues compared to their control counterparts[36, 54].

PGRN further demonstrates its protective attributes in the context of sepsis and endotoxic shock, conceivably by modulating cytokines[55], transcription factors, and immune cell apoptosis[56]. Findings from various animal studies have indicated that deficiency in PGRN exacerbates the severity of sepsis. Although PGRN holds promise as a prospective therapeutic

target, a comprehensive elucidation of its underlying mechanisms continues to be a persistent and evolving research pursuit[20, 41, 55, 57-59].

In the context of renal function, the administration of rPGRN has demonstrated the ability to ameliorate the impact of renal ischemia/reperfusion injury (IRI) by mitigating hypoxia-induced inflammation[60]. In cases of acute kidney disease (AKI), PGRN levels are diminished, within the kidneys, concomitant with elevated levels of serum creatinine, blood urea nitrogen, heightened morphological damage, and increased inflammation[60-62].Moreover, recent investigations have unveiled PGRN's emerging role in preserving mitochondrial homeostasis in podocytes in diabetic nephropathy (DN), thereby suggesting its potential as an innovative therapeutic approach for managing patients afflicted with DN, IRI and AKI[63].

While numerous studies underscore PGRN's anti-inflammatory attributes, a different narrative unfolds in the chronic setting of obesity and insulin-resistant diabetes[64]. In these chronic conditions, elevated PGRN levels have been linked to impaired glucose metabolism and low-grade inflammation. Intriguingly, mice deficient in PGRN are afforded protection from high-fat-diet-induced obesity and insulin resistance. Furthermore, clinical evidence correlates increased PGRN levels in human subcutaneous adipose tissue and serum with obesity, type 2 diabetes, and dyslipidemia[65, 66]. This connection is reinforced by the observation that heightened PGRN levels hinder insulin signaling and glucose uptake, potentially contributing to the development of insulin resistance in the context of obesity[67, 68]. It is worth noting that PGRN's roles may vary within different tissues, cells, and metabolic scenarios, which adds to the complexity of its function. Additionally, it is crucial to differentiate between PGRN and its proteolytically derived peptides, known as granulins. While PGRN exhibits trophic properties and anti-inflammatory potential, granulins resemble inflammatory mediators akin to cytokines[69]. This underscores the

intricate and context-dependent nature of PGRN, where its regulatory proteolysis and subsequent generation of pro-inflammatory granulin peptides dictate its ultimate inflammatory or anti-inflammatory role.

While the function of PGRN has been the subject of scrutiny in both physiological and diverse pathophysiological contexts, the precise mechanisms through which PGRN modulates cellular biology remain a topic of debate and remain incompletely understood. In our present study, we are elucidating novel pathways through which PGRN exerts control over VSMC contractility. This control is achieved by orchestrating mitochondrial quality through the regulation of mitochondrial recycling processes and redox signaling, emphasizing the innovative and crucial role of PGRN in this particular context.

1.5 Progranulin and Mitochondria

Mitochondria are vital organelles distinguished by their double-membrane structure, including the outer mitochondrial membrane (OMM) and the inner mitochondrial membrane (IMM). They play a critical role in cellular processes, with a primary focus on energy production through oxidative phosphorylation (OXPHOS)[70]. The IMM encapsulates a crucial compartment referred to as the matrix, while the intermembrane space, located between the IMM and OMM, also plays a pivotal role in various cellular processes.[71, 72]. The IMM is the primary site for oxidative phosphorylation, encompassing components such as the electron transport chain and a range of channels. Notably, these channels include the mitochondrial Ca2+ uniporter and the inner membrane anion channel[73, 74]. The OMM has a distinct protein composition. These proteins encompass pore-forming components, enzymes, and proteins that actively participate in the

intricate processes of mitochondrial fission and fusion[75, 76]. Mitochondria serve as the primary energy generators within the cell, producing ATP through two main processes: the Krebs cycle in the matrix and oxidative phosphorylation facilitated by the five electron transport chain complexes embedded in the IMM[77, 78].The electrochemical gradient across the IMM plays a critical role in ATP synthesis, a process facilitated by ATP synthase, also referred to as Complex V. Any disruption or depolarization of the mitochondrial membrane potential can have far-reaching effects, influencing a wide range of essential functions and often serving as a reliable indicator of mitochondrial dysfunction[79]. Mitochondria, as highly dynamic organelles, participate in a continuous interplay of biogenesis, fission, fusion, and mitophagy processes. Biogenesis, creates new mitochondria to meet cellular energy demands and sustain function[80], is intricately interconnected with mitochondrial dynamics, encompassing fission (division) and fusion (merging). These dynamic processes meticulously govern the number, morphology, and overall functionality of mitochondria within a cell[81].

Simultaneously, mitophagy is a selective process designed to eliminate damaged mitochondria, ensuring cellular health and homeostasis. The seamless coordination of these biogenesis and mitophagy mechanisms holds paramount importance in preserving mitochondrial function. Notably, mitochondrial dysfunction is closely linked to the aging process[82] and immune responses[83], contributing to various diseases, such as cancer[84], neurodegenerative disorders[85], and cardiovascular conditions[86]. Given the pivotal roles played by mitochondria, maintaining mitochondrial homeostasis is a critical aspect of overall cellular well-being. Our study has unveiled the role of PGRN in regulating mitophagy, thereby influencing VSMC contractility.

Mitophagy

Mitophagy, denotes the autophagy-dependent degradation of mitochondria, a cellular phenomenon wherein mitochondria are enveloped within membrane-bound vesicles, commonly termed autophagic vacuoles or autophagosomes, with the ultimate intent of subsequent degradation and recycling in the lysosomes[87, 88]. Its primary objective is to uphold optimal cellular energy production by selectively identifying and breaking down impaired mitochondria, preventing the production of toxic molecules, such as reactive oxygen species (ROS). Mitophagy involves two key proteins, E3 ubiquitin ligase Parkin (Parkin), and PTEN-induced serine/threonine kinase 1(PINK1). Under normal, steady-state conditions, PINK1 continually enters the mitochondria, where it undergoes cleavage by mitochondrial proteases. The cleaved PINK1 is then retro transported to the cytosol, where it is degraded through the N-end rule pathway via the ubiquitin proteasome system, resulting in very low detectable levels of PINK1 in healthy cells[89].Conversely, Parkin, a cytosolic protein, becomes active on the OMM. It translocates to damaged mitochondria as a pivotal component of the mitochondrial degradation process[90, 91].

Dysregulation of mitochondrial dynamics and impaired mitophagy in VSMCs, leading to an overproduction of ROS, has been associated with VSMC senescence and the potential acceleration of vascular aging, as demonstrated in mouse models[82] and clinical studies[92].VSMCs from atherosclerotic lesions display dysregulated mitophagy and a substantial decrease in mitochondrial respiration compared to VSMCs from disease-free arteries[93, 94].Furthermore, mitochondrial dysfunction in VSMCs contributes to the development of aortic aneurysms, as observed in conditions like Marfan syndrome (MFS)[95]. In non-heritable aortic aneurysms and dissections induced by atherosclerosis, there is a decline in mitochondrial respiration, impaired mitochondrial biogenesis, and a reduction in mitochondrial proteins in

VSMCs from both mouse and human aortic aneurysms[96-98].In cases of hypertension, there is an accumulation of dysfunctional and ROS-producing mitochondria[99, 100]. Prior investigations have explored PGRN's involvement in mitochondrial biogenesis and mitophagy. These studies notably revealed that PGRN deficiency exacerbated mitochondrial impairment and dysfunction within the podocytes of diabetic mice[63]. Moreover, PGRN played a protective role in primary rat cortical neurons by preventing hyperglycemia-induced reductions in mitophagy[101].

In our current study, we are not only uncovering the influence of PGRN on VSMC contractility but also gaining insights into how PGRN governs mitochondrial dynamics and mitophagy within VSMCs. Significantly, our research is delving deeper, revealing that these effects are orchestrated by a compromised lysosome quality and a disturbance in biogenesis equilibrium.

1.6 Progranulin and Lysosomes

To ensure an efficient mitochondrial recycling process, the presence of high-quality lysosomes is imperative. Lysosomes, are membrane-bound organelles, that house enzymes which break down a variety of macromolecules and organelles through the formation of autophagosomes[102].It's noteworthy that diseases linked to the loss of PGRN function are categorized as lysosomal diseases. This association arises because the lysosomal transmembrane glycoprotein TMEM106b, which has been identified as a genetic modifier of PGRN expression. Genome-wide association studies (GWAS) have identified single nucleotide polymorphisms (SNPs) in or near TMEM106b that impact the age of onset of FTLD[103]. Elevated levels of TMEM106B are correlated with the enlargement of lysosomes. Moreover, the complete knockout

of PGRN has been linked to NCL, a lysosomal storage disorder characterized by the intracellular accumulation of ceroid lipofuscin in neurons due to impaired lysosomal degradation[104, 105].

These combined findings have led to a better understanding of PGRN's implications within the lysosome, making the regulation of lysosomal activity a central focus in therapeutic research[106]. In different model organisms such as *C. elegans* and zebrafish, the absence of PGRN has been linked to observable changes in lysosomal dynamics. For example, in *C. elegans*, it results in the formation of smaller yet more numerous lysosomes[107], while in zebrafish, it leads to a reduction in the length of neuronal axons and an amplified negative impact of TDP-43[108, 109]. Similarly, mice lacking PGRN show elevated levels of lysosome associated membrane protein 1 (LAMP1), a recognized lysosomal marker, indicating a potential accumulation of lysosomes[110-112]. Furthermore, PGRN's binds Cathepsin-D (CTSD), an essential lysosomal protease[113]. Interestingly, the absence of CTSD also results in NCL, underscoring the critical nature of this regulation in lysosomal biology[114]. PGRN appears to play a role in promoting the maturation of CTSD, thereby enhancing its enzymatic activity[115-117].The linkage among these diverse mechanisms, encompassing cathepsin activity[104, 116], acidification[114, 118], and the indirect indications of PGRN's potential role in lysosomal lipid catabolism[119-121], is further underscored by the association between PGRN and the lysosomal transmembrane glycoprotein TMEM106b[122, 123]. Moreover, the observed repercussions of PGRN deficiency on glycosphingolipid metabolism imply that PGRN may indeed serve broader functions within the lysosomal membrane[124, 125]. Nevertheless, the precise mechanism by which PGRN regulates lysosomal activities remains to be fully elucidated.

1.7 Regulation of Vascular Smooth Muscle Phenotype

The regulation of vascular smooth muscle cell (VSMC) phenotype is a complex process crucial for maintaining vascular function. VSMCs possess a remarkable ability to adapt between two primary phenotypes: synthetic and contractile. These distinct states play pivotal roles in vascular homeostasis, repair, and pathophysiology.

The contractile phenotype is characterized by a differentiated state optimized for force generation and maintenance of vascular tone. These cells exhibit a spindle-shaped morphology with well-developed contractile apparatus, enriched in contractile proteins such as smooth muscle alpha-actin (α-SMA) and myosin heavy chain[126]. Contractile VSMCs actively regulate blood vessel diameter, responding to various stimuli, including vasoconstrictors (e.g., endothelin-1) or vasodilators (e.g., nitric oxide), to modulate blood flow and pressure[3].

Conversely, the synthetic phenotype is associated with a more proliferative and secretory nature[127]. These VSMCs adopt a synthetic state in response to injury or during vascular remodeling. In this state, cells exhibit increased synthetic activity, producing extracellular matrix components like collagen and elastin, as well as growth factors and cytokines. This phenotype contributes to repair processes but, when dysregulated, can lead to pathological conditions like atherosclerosis and restenosis after angioplasty[4].

The transition between these phenotypes is tightly regulated by various signaling pathways and factors. Key regulators include growth factors (e.g., platelet-derived growth factor, transforming growth factor-beta)[128], transcription factors (e.g., serum response factor, myocardin)[129], and microRNAs, which orchestrate gene expression changes driving phenotype switching[130].

Environmental cues also play a crucial role. Mechanical forces, such as changes in blood pressure and shear stress, influence VSMC phenotype[131]. Additionally, inflammatory mediators and metabolic factors within the vessel wall impact phenotype regulation, contributing to vascular diseases' development and progression[132].

Understanding the intricate balance between these phenotypes is crucial for developing therapeutic strategies targeting vascular disorders. Strategies aimed at maintaining VSMCs in a contractile state or modulating their transition to a synthetic phenotype hold promise in preventing or treating vascular diseases, ultimately preserving vascular function and health.

1.8 Progranulin and Cardiovascular Diseases

PGRN has emerged as a noteworthy regulator in the realm of cardiovascular biology, though this area of study remains relatively underexplored. Notably, the absence of PGRN has been associated with several adverse cardiovascular outcomes, including accelerated cardiac aging, characterized by cardiac hypertrophy and eventual heart failure[133]. In addition, PGRN deficiency has been linked to exacerbated cardiac and renal injuries induced by hyperhomocysteinemia diet[134] and decreased survival rates and an increased presence of cardiac fibrosis following a myocardial infarction (MI)[135].In contrast, within the same study, when rPGRN was administered in experimental models, such as permanent left coronary artery occlusion (LCA) in mice and myocardial ischemia-reperfusion (I/R) in rabbits, it resulted in decreased infarct size, reduced neutrophil infiltration, and improved cardiac function[136].

Along with cardiac injury, deficiency in PGRN was found to exacerbate atherosclerosis in mouse models. Firstly, an apolipoprotein E (ApoE) and PGRN double KO mice, display an

increased formation of atherosclerotic lesions[137]. Furthermore, ApoE mice deficient for PGRN only in the hematopoietic compartment (chimeric mice) demonstrate exacerbated vascular inflammation and atherosclerotic plaque[134]. Together, these findings suggest that PGRN might orchestrate the immune system in atherosclerosis development, but its participation in regulating the vascular biology is still to be fully elucidated.

Within vascular endothelial cells, PGRN demonstrates significant anti-inflammatory characteristics that confer athero-protective benefits. These advantages encompass the enhancement of nitric oxide (NO) levels and the inhibition of NFκB, thereby preserving endothelial integrity in isolated cells[138]. These effects ultimately contribute to the effective regulation of vascular tone of mesenteric arteries with intact endothelium and blood pressure control, as recently demonstrated in research conducted by our team[139].

The relationship between PGRN and vascular VSMCs remains understudied, with limited research on the role of PGRN in VSMCs. However, as demonstrated by immunohistochemical analysis of human carotid endoatherectomy specimens, VSMCs express PGRN in the intima layer. *In vitro*, overexpression of PGRN attenuates TNFα-induced VSMCs migration and IL-8 production, in contrast suppression of PGRN exacerbates TNFα effects, suggesting that PGRN may play a role in sustaining proper vascular biology[140]. Additionally, PGRN levels are elevated in calcified human aortic valves, suggesting that it might serve as a protective mechanism against valve fibrosis and osteoblastic differentiation, since intact PGRN attenuates the calcification *in vitro*[141].

While there has been prior research establishing a link between PGRN and VSMCs, a crucial question remains unanswered: Does PGRN influence vascular contractility, a pivotal event

in the context of CVDs? Furthermore, the specific mechanisms through which PGRN operates within VSMCs have yet to be fully elucidated.

To address these gaps in our understanding, our study is designed to explore the intricate mechanisms by which PGRN regulates VSMC biology. We aim to uncover how PGRN impacts mitochondrial dynamics and mitophagy, as well as its role in maintaining lysosomal quality. This investigation pioneers the concept that PGRN is not only associated with but is indeed indispensable for preserving the proper function of VSMCs, particularly in terms of vascular contractility. By shedding light on these mechanisms, our research aims to contribute significantly to our knowledge of PGRN's role in cardiovascular health.

1.9 Aims

In summary, the impairment of vascular contractility and the occurrence of mitochondrial dysfunction are pivotal factors in the development of CVDs. One of the significant challenges in reducing the prevalence of cardiovascular morbidity and mortality is our limited understanding of the intricate vascular mechanisms and the associated risk factors that underlie the development of cardiovascular conditions. Currently, the precise mechanisms by which PGRN, an anti-inflammatory protein, regulates mitochondrial homeostasis and vascular contractility remain unknown. In my research, I have used *in vivo* animal models of PGRN deficiency and *in vitro* primary VSMCs derived from the aorta of both wild-type and global PGRN KO mice combined with pharmacological approaches to rescue mitophagy and model of vascular dysfunction, Angiotensin-II treated mice.

The goal of my research is to expand our understanding of how PGRN regulates vascular physiology with a major focus on understanding the connection between PGRN and mitochondrial function, an area that lacks comprehensive understanding. Upon the completion of these studies, I will provide insights into the importance of PGRN modulating VSMC biology, as well as the potential mechanisms by which PGRN is a master regulator of mitochondrial function.

We hypothesize that PGRN maintains the VSMC homeostasis by regulating mitochondrial quality and keeping a physiological mitochondria-dereived reactive oxygen species (mROS) levels (Theoretical framework)**.** We will test this hypothesis in the following two aims.

AIM 1: Determine whether PGRN controls VSMC profile by regulating oxidative phosphorylation and mitophagy process. Our pilot data demonstrate that lack of PGRN leads to a dysfunctional mitochondrion associated with exacerbated mROS production. We will use PGRN deficient VSMC (PGRN-/-), pharmacological tools [antioxidant agents, and autophagy/mitophagy modulators], as well as genetic manipulations (loss or gain of PGRN function in VSMC) to characterize the cellular mechanisms in the context of vascular proliferation and migration.

AIM 2: Investigate whether reduced vascular PGRN levels facilitate the genesis and progression of pathological vascular remodeling. Our preliminary data indicate that arteries and VSMC from PGRN-/- are prone to injury. We will use different pharmacological treatments, as well as PGRN-lentivirus to dissect the cellular mechanisms.

We expect to demonstrate: 1) PGRN is a master regulator of vascular homeostasis; 2) Loss of PGRN facilitates vascular injury; 3) PGRN maintains mitochondrial quality via regulating mitophagy, complex I, and mROS production.

2.0 Chapter 2: Adjusted Vascular Contractility Relies on Integrity of Progranulin Pathway: Insights into Mitochondrial Function

Disclosure: This chapter has been adapted from the following paper under consideration for publication-

Singh, S., Bruder-Nascimento, A., Costa, C.M., Alves, J.V., Sivakama, B.S., Goetzman, E.S., Bruder-Nascimento, T**.** Adjusted vascular contractility relies on integrity of progranulin pathway: Insights into mitochondrial function.

2.1 Introduction

Cardiovascular diseases (CVDs) encompass a wide range of conditions affecting the heart and blood vessels, and in 2020, they were responsible for approximately 19.1 million global deaths[2]. These conditions can be congenital, acquired, or have a hereditary component[142]. VSMC, primarily found in arterial walls, typically adopt a quiescent, contractile state to regulate vascular tone, a crucial process in CVDs. However, in CVDs, VSMC transition to a synthetic phenotype, losing their contractile properties and contributing to arterial wall dysfunction, furthering the progression of CVDs[143]. Therefore, strategies aimed at preserving VSMC contractility hold promise for CVDs treatment.

Recent research suggests that mitochondrial dysfunction plays a central role in the development and progression of CVDs and its associated complications[144]. Mitochondrial dysfunction contributes significantly to the phenotypic shift in VSMC[145]and the development of arterial dysfunction[146, 147]. In CVDs, mitochondrial dysfunction leads to the generation of reactive oxygen species (mtROS) and decreased ATP production, resulting in VSMC contractile impairment. However, the precise mechanisms underlying mitochondrial functions in VSMCs remain largely unknown. Therefore, there is a pressing need to explore innovative therapeutic and preventive strategies focused on revitalizing VSMC mitochondrial function. This endeavor involves targeting key components responsible for maintaining mitochondrial homeostasis, including mitochondrial fission, fusion, biogenesis, and mitophagy. Disruptions in these intricate mechanisms can lead to mitochondrial dysfunction and subsequent organ damage. Particularly in the context of CVDs, deviations in mitochondrial structure and function are associated with reduced levels of mitophagy, emphasizing the potential importance of mitophagy in sustaining mitochondrial homeostasis and preserving VSMCs function[148, 149]. PGRN, a secreted

glycoprotein, is widely expressed in various tissues and cell types, with diverse roles encompassing embryogenesis, inflammation, wound healing, neurodegenerative processes, and lysosomal function[150]. Heterozygous mutations in the granulin (GRN) gene result in PGRN protein haploinsufficiency, leading to neurodegeneration in frontotemporal lobar degeneration (FTLD)[151]. PGRN protects cardiac and renal integrity during ischemia-reperfusion injury[63, 136]. Furthermore, PGRN demonstrates anti-inflammatory effects in the vascular endothelium, conferring athero-protective benefits such as increasing nitric oxide (NO) levels[138], preserving endothelial integrity, and regulating blood pressure (BP), as recently demonstrated by our research group[139]. In VSMCs, PGRN acts as a mitigator of calcification[141]and a regulator of cell migration through its modulation of IL-8 secretion[152]. Although previous studies have described the vascular protective effects of PGRN in other contexts, its role in regulating vascular contractility remains unclear.

This study unveils a novel aspect of PGRN's function, showing that PGRN deficiency decreases VSMCs contractility. Importantly, our findings reveal that PGRN plays a critical role in preserving mitochondrial equilibrium by modulating mtROS signaling, mitochondrial complex I biogenesis and function, and mitophagy flux in VSMCs. This discovery suggests that PGRN may offer a highly promising therapeutic avenue for addressing CVDs by modulating mitochondrial function and cellular bioenergetics. Furthermore, it implies that individuals with PGRN deficiency may face cardiovascular risks in addition to neurodegenerative diseases.

2.2 Materials and Methods

2.2.1 Mice

Twelve- to sixteen-week-old male and female C57BL6/J wild type (PGRN+/+), global PGRN mutant B6(Cg)-Grntm1.1Aidi/J (PGRN-/-), and male mt-Keima mice were used. All mice were fed with standard mouse chow and tap water was provided ad libitum. Mice were housed in an American Association of Laboratory Animal Care–approved animal care facility in the Rangos Research Building at the Children's Hospital of Pittsburgh of the University of Pittsburgh. The Institutional Animal Care and Use Committee approved all protocols (IACUC protocols # 19065333 and 22061179). All experiments were performed in accordance with Guide Laboratory Animals for The Care and Use of Laboratory Animals.

2.2.2 Lentivirus Encoding PGRN Delivery in Fresh Aortae

Lentiviral particles (LV) were packaged and transfected by Vectorbuider as pLV[Exp]-Puro-CMV>mGrn[NM_008175.5] with murine phosphoglycerate kinase (mPGK) promotor. The thoracic aortae from both PGRN+/+ and PGRN-/- mice were aseptically isolated and subsequently rinsed with PBS. Following this, they were placed in individual wells of a 96-well plate, each containing 100 µL of Dulbecco's Modified Eagle Medium (DMEM). The aortae were then categorized into two groups: control and treatment with LV. In the treatment wells, 1 µL of a 106 LV vector was added. The entire culture plate was placed in a 37°C incubator with a 5% CO2 atmosphere for a duration of 24 hours.

After this 24-hour incubation period, the aortae were again washed with PBS to remove any residual substances. They were subsequently employed for various analyses, including western blot analysis, myography, and oxygen consumption rate (OCR) experiments.

2.2.3 Vascular Function

Thoracic aortic rings were utilized in our experiments and mounted in a wire myograph (Danysh MyoTechnology) for isometric tension recordings, employing PowerLab software (AD Instruments) as previously described in the literature[153, 154]. Briefly, rings measuring 2mm in diameter were dissected from the thoracic aorta, and the endothelium was removed by using a needle 25G. Aortic rings were carefully placed in tissue baths containing Krebs Henseleit Solution, which was maintained at a temperature of 37 °C and continuously aerated with a mixture of 95% O2 and 5% CO2. The composition of the Krebs Henseleit Solution was as follows (in mM): 130 NaCl, 4.7 KCl, 1.17 MgSO4, 0.03 EDTA, 1.6 CaCl2, 14.9 NaHCO3, 1.18 KH2PO4, and 5.5 glucose.

Protocol to Study if the Deficiency in the PGRN affects Vascular Contractility

KCL (120mM)-induced contractility and concentration response curve (CRC) to phenylephrine (PE, alpha-1 adrenergic receptor-dependent vasoconstrictor) and U46619 [thromboxane A2 (TXA2) mimetic] were analyzed in endothelium-denuded rings from thoracic aorta from PGRN+/+ and PGRN-/- mice.

***Ex vivo* Protocol for Regain of PGRN Function in Isolated Aortae**

Aortae were harvested from PGRN+/+ and PGRN-/- mice, the endothelium was removed, rings (2 mm) were isolated, and endothelium was removed as described above. Then, rings were incubated with LV encoding PGRN (10^6/mL) for 24 hours in DMEM containing 100 U/ml

penicillin, 100 μg/ml streptomycin, and 10 mmol/L Hepes. Re-expression of PGRN in aortae from PGRN-/- or overexpression of PGRN in aorta from PGRN+/+ were confirmed by western blot.

2.2.4 High-Resolution Respirometry

To investigate the impact of PGRN on mitochondrial function, we used Oroboros Oxygraph-2K (Oroboros, Österreich, Austria) (Doerrier et al., 2018). Aortas from PGRN+/+ and PGRN-/- were freshly isolated, carefully dissected, weighed, and placed into 500 μL of isolation buffer composed of 225 mM mannitol, 75 mM sucrose, 10 mM Tris pH 7.4, and 0.2 mM EDTA. The aortas were then transferred to O2-equilibrated chambers containing 5 mL of isolation buffer. Once the baseline became stable, 10 μM cytochrome C (Sigma, St. Louis, MO) was introduced to assess mitochondrial integrity.

To evaluate mitochondrial respiration, a series of substrates and inhibitors were added sequentially. Specifically, malate (5 mM, Sigma, St. Louis, MO), ADP (2 mM, Sigma-Aldrich Co., St. Louis, MO), pyruvate (5 mM, Sigma-Aldrich Co.), glutamate (5 mM, Sigma-Aldrich Co.), and succinate (5 mM, Sigma-Aldrich Co.) were successively administered to stimulate State 3 respiration. State 3 respiration is often used in research to assess the capacity of mitochondria to produce ATP under conditions of high energy demand[155, 156]. To uncouple the electron transport chain (ETC), carbonyl cyanide m-chlorophenyl hydrazone (CCCP) (1mM, Sigma-Aldrich Co.) was added. Finally, to inhibit complex I, Rotenone (1mM, Sigma, St. Louis, MO) was introduced to halt mitochondrial respiration entirely[157].

2.2.5 Vascular Remodeling

Mice were euthanized to obtain aortae, followed by perfusion with chilled phosphate-buffered saline (PBS). Harvested aortae were then immersed in a 4% paraformaldehyde (PFA) solution for histological examination. After 12 hours in PFA, the tissues were transferred to 70% ethanol, where they remained until sample preparation for histology. The aortae were embedded in paraffin, after which the samples were sectioned and subjected to hematoxylin and eosin (H&E) and Masson's trichrome staining to evaluate vascular remodeling and structural characteristics.

2.2.6 Pharmacological Interventions in Mice

Restoration of circulating PGRN: To restore circulating PGRN levels, PGRN+/+ and PGRN-/- mice were subjected to a 7-day treatment regimen using rPGRN delivered through ALZET osmotic minipumps (Alzet Model 1001; Alzet Corp Durect, Cupertino, CA) at a rate of 20ug/day, following established protocol by our group. After this 7-day treatment period, we conducted the analysis of mitochondrial respiration employing Oroboros O2k respirometry.

Autophagy Inducer

Spermidine, recognized as a natural polyamine with autophagy-stimulating properties[158] was employed in this study. Both PGRN+/+ and PGRN-/- mice were randomly allocated into two cohorts: the spermidine treatment group and the control group. The treatment group received a 14-day regimen of spermidine administered via their drinking water at a concentration of 3mM. After this 14-day treatment period, evaluations were conducted, including the assessment of vasocontraction responses in thoracic aortas and the analysis of mitochondrial respiration

employing Oroboros O2k respirometry. In addition, hearts were harvested for further analysis of autophagy marker through western blotting.

Angiotensin II Infusion

Both PGRN+/+ and PGRN-/- mice were subjected to a 14-day infusion protocol using ALZET osmotic minipumps (Alzet Model 1002; Alzet Corp Durect, Cupertino, CA) to delivery Angiotensin-II (Ang-II) at a dose of 490 ng/min/kg [139, 159]. Subsequently, thoracic aortas were utilized for a series of experiments, including assessments of vascular reactivity, histological analyses, and mitochondrial respiration.

2.2.7 Fresh Primary VSMCs Isolation from Thoracic Aorta

We conducted the isolation of VSMCs from the aortas of male PGRN+/+ and PGRN-/- mice. The isolation procedure followed a well-established enzymatic dissociation protocol[160-163]. Following the isolation, the aortic smooth muscle cells were cultured in DMEM from Invitrogen Life Technologies. To maintain cell health and preserve their physiological characteristics, the culture medium was supplemented with 10% fetal bovine serum (FBS) obtained from HyClone, along with 100 U/ml penicillin, 100 µg/ml streptomycin, and 10 mmol/L Hepes (pH 7.4) from Sigma-Aldrich. To ensure the viability and functionality of the arterial smooth muscle cells during experimentation, we utilized cells within passages 4 to 8 [164].

2.2.8 Rat Aortic Smooth Muscle Cells

Rat Aortic Smooth Muscle cells (RASMC) (Lonza, Walkersville, MD) and meticulously maintained in DMEM (Gibco from Thermo Fisher Scientific, Waltham, MA, U.S.A)

supplemented with 10% FBS (HyClone Logan UT, U.S.A), 100 U/ml penicillin, and 100 µg/ml streptomycin (Gibco from Thermo Fisher Scientific, Waltham, MA, U.S.A) as described before[165].

2.2.9 VSMCs Overexpressing PGRN via Lentiviral Transduction in Rat Aortic Smooth Muscle Cells (aSMC)

Lentiviral particles (LV) were packaged and transfected by Vectorbuider as pLV[Exp]-Puro-CMV>mGrn[NM_008175.5] with mPGK promotor. One day prior to infection, 1×105−2×105 selected aSMC per well were seeded in a six-well plate, ensuring they reach an approximate confluency of 80% before initiating infection. On Day 1, the pre-existing media was aspirated, and each well was supplemented with 400 ul of fresh media, along with 5 ul of Polybrene at a concentration of 8 µg/mL as a transfection enhancer. Furthermore, 1 ul of LV containing 1x106 viral particles is added to each of the wells. Control wells, one containing only cells and the other with media alone, were also maintained. The cells were subsequently incubated for a period of 48 to 72 hours without changing the media. On Day 3, the media was exchanged with 2 ml of DMEM supplemented with Puromycin at a concentration of 10 ug/ml. The introduction of Puromycin is delayed by at least 24 hours post-infection to ensure adequate expression of the Puromycin resistance gene. Day 4 entails the removal of media, which was preserved at -20°C for future use, followed by its replacement with fresh DMEM containing Puromycin at a concentration of 5 ug/ml. Finally, on Day 5, the media is once again replaced with DMEM containing Puromycin at 5 ug/ml. Throughout this procedure, special attention was directed towards monitoring the positive control well, as it had the potential to exhibit cell death in contrast to the LV-infected cells. The cells were then washed with phosphate-buffered saline (PBS) and incubated in regular medium for

48 h, after which PGRN expression was confirmed by western blot in cell lysate and ELISA (R&D biosystem) in the supernatant of aSMC (control) and aSMC^{PGRN} (high expression of PGRN). All cell culture processes were diligently conducted under conditions of 5% CO2 at 37°C, with the experiments thoughtfully executed in triplicate to ensure robustness and reliability of the results.

2.2.10 Pharmacological Treatments in Cells

In our experimental setup, we employed specific treatments to investigate the autophagy pathway, mitochondrial ROS, and detrimental pathways. Bafilomycin (50 μM), was used as an inhibitor of autophagosome-lysosome fusion to confirm the ability of PGRN to induce autophagy. Recombinant PGRN (rPGRN) (600ng/mL) was used to examine if circulating PGRN regulates mitochondria respiration. Cells were also treated with Platelet-Derived Growth Factor-BB (PDGF) (100 ng/ml) to analyze where PGRN deficient cells are more sensitive to a deleterious environment. Antimycin A (20 μM) was used to induce mtROS formation.

2.2.11 Collagen Contraction Assay

To assess the contractility of VSMCs, a collagen gel contraction assay was conducted [166]. In the gel preparation process, 50 μL of 100 mM/L NaOH was added to 400 μL of rat tail collagen (PurColl, Advanced Biomatrix, #5005) kept on ice. This was followed by the addition of 50 μL of 10×PBS. Subsequently, 280 μL of VSMCs suspension (1.2×105 cells/ML) was introduced to form the gel-cell mixture, which was then transferred to the wells of a 12-well plate and allowed to further incubate for 30 minutes at 37 ℃[167]. A negative control lacking cells was also established. After gelation, 500 μL of culture medium was added to each well. The

VSMC/collagen gel was left to float freely by gently scraping with a cell scraper. Contraction extent was evaluated by measuring gel area and diameter immediately (baseline) and every 24 hours using a dissection microscope. The plates were then placed back in an incubator at 5% CO2 and 95% air. All experiments were carried out in triplicate over a 72-hour period. For data analysis, the ImageJ imaging analysis software (National Institutes of Health, Bethesda, MD) was employed to measure the gel area. The final data was presented as mean ± SEM with triplicate wells in each group, and the data was reported in terms of area in mm^2.

2.2.12 Phalloidin Fluorescence

Phalloidin fluorescence was employed for visualizing the cellular cytoskeleton [165]. Cells were cultured on coverslips overnight. Subsequently, they were fixed using a 3.7% formaldehyde solution in PBS for 15 minutes at room temperature. Permeabilization was accomplished by treating the cells with 0.1% Triton™ X-100 in PBS for 15 minutes. A blocking step followed, involving a solution containing 1% BSA for 45 minutes at room temperature. The cells were then exposed to a phalloidin staining solution for 60 minutes at room temperature. Throughout the process, residual solutions were removed through PBS washes. DAPI staining was employed for visualizing cell nuclei. Microscopic imaging was conducted using a fluorescence microscope (Revolve, Echo, San Diego, California, USA).

2.2.13 Seahorse Extracellular Flux Assay

The sensor cartridge and utility plate (Agilent, Santa Clara, CA) were hydrated and prepared according to company protocol. Primary VSMCs (2x104-3x104) were seeded onto to an

Xfe96 poly-D-Lysine (PDL) Cell Culture Plate (Agilent) in 80uL of 5% FBS, 1% pen/strep complete DMEM (Sigma, St. Louis, MO) and incubated for 1 hour at room temperature for cell adhesion. Complete DMEM was removed and replaced with 180uL of Xfe DMEM Medium, pH 7.4 (Agilent) supplemented with 25mM D-(+)-Glucose (Sigma), 1mM Sodium Pyruvate (Sigma), and 2mM L-Glutamine (Corning, Corning, NY) and incubated in a non-CO2 37oC incubator for an additional 1 hr. Seahorse XF Cell Mito Stress Test Kit (Agilent, Santa Clara, CA) Oligomycin (Oli), carbonyl cyanide-p-trifluoromethoxy phenylhydrazone (FCCP), and Rotenone(ROT) reagents were reconstituted in 420 uL and 720 uL of XF Assay Media (Agilent), respectively. Each reagent was loaded into its respective port in sensor cartridge for a final well concentration of 1.0 uM Oli (ATP synthase inhibitor), 1.0 uM FCCP (uncoupling agent), and 0.5 uM ROT (complex I inhibitor)[168]. The sensor cartridge was loaded into XF96 Seahorse Extracellular Flux Analyzer (Agilent) for sensor calibration followed by addition of cell culture plate. The data were analyzed using Xfe software 2.6.1 (Agilent Technologies, Inc.) and normalized to the amount of protein loaded per well.

2.2.14 Real-Time Polymerase Chain Reaction (RT-PCR)

mRNA extraction from aortae and VSMC was accomplished using the Rneasy Mini Kit (Qiagen, Germantown, MD, USA). To synthesize complementary DNA (cDNA), reverse transcription polymerase chain reaction (RT-PCR) was performed utilizing SuperScript III (Thermo Fisher, Waltham, MA, USA). The reverse transcription process occurred at 58 ºC for 50 minutes, succeeded by enzyme inactivation at 85 ºC for 5 minutes. For real-time quantitative RT-PCR, the PowerTrack™ SYBR Green Master Mix (Thermo Fisher, Waltham, MA, USA) was employed. The gene sequences utilized are provided in the Supplementary Table 1. Experiments

were conducted on a QuantStudio™ 5 Real-Time PCR System using a 384-well format (Thermo Fisher, Waltham, MA, USA). Data analysis was executed using the 2ΔΔCt method, with results represented as fold changes signifying either upregulation or downregulation.

2.2.15 Immunoblotting (Western Blot)

Aortic protein extraction was carried out using a radioimmunoprecipitation assay (RIPA) buffer (Thermo Fisher Scientific Inc.), supplemented with protease inhibitor cocktail (Roche), which consisted of 30 mM HEPES (pH 7.4), 150 mM NaCl, 1% Nonidet P-40, 0.5% sodium deoxycholate, 0.1% sodium dodecyl sulfate, 5 mM EDTA, 1 mM NaV04, 50 mM NaF, 1 mM PMSF, 10% pepstatin A, 10 μg/mL leupeptin, and 10 μg/mL aprotinin. Total protein extracts obtained from aortic homogenates were subjected to centrifugation at 15,000 rpm for 10 minutes, and the resulting pellet was discarded, 25 μg of protein was used. For aVSMC and rat aSMC samples, direct homogenization was performed using 2x Laemmli Sample Buffer supplemented with 2-Mercaptoethanol (β-mercaptoethanol). Protein samples (were separated by electrophoresis on a polyacrylamide gradient gel, and subsequently transferred to a PVDF membrane (Immobilon FL, EMD Millipore, Billerica, MA). To prevent non-specific binding, the membranes were blocked with either 5% skim milk or 1% bovine serum albumin (BSA) in tris-buffered saline solution with tween for 1 hour at 24 ºC. Specific antibodies, as listed in supplementary table 2, were then applied to the membranes, and incubated overnight at 4 ºC. Following the primary antibody incubation, secondary antibodies were used, and the membranes were subjected to enhanced chemiluminescence with a luminol reagent (SuperSignal™ West Femto Maximum Sensitivity Substrate, Thermo Fisher Waltham, MA, USA) was used for antibody detection.

2.2.16 Mitochondrial Related Experiments

Complexes Expression-OXPHOS

We employed the OXPHOS cocktail antibody mixture (Abcam), specifically designed to target complexes subunits within the Oxidative Phosphorylation (OXPHOS). To ensure the preservation of these hydrophobic protein's integrity, a meticulous methodology was adhered to. Prior to initiation, cells were collected and lysed for protein extraction, with utmost care taken to maintain the integrity of OXPHOS complexes. Samples were strictly kept unheated before their application onto the gel.

Mitochondrial Complex I Activity

The assessment of mitochondrial respiratory chain complex I activity was conducted by using the specialized Complex I Enzyme Activity Assay Kit (ab109721). Initially, cells were lysed, and extracts from these cells were carefully loaded onto a microplate. Subsequently, the plate wells were meticulously washed three times with a designated buffer. Following this preparation, 200 µL of assay solution was added to each well, and the optical density (OD450 nm) was measured in kinetic mode at room temperature for up to 30 minutes (SpectraMax i3x Multi-Mode Microplate Reader). Absorbance was analyzed at OD 450 nm, which was used as an indicator of Complex I activity.

NAD+/NADH Assay

The NAD+/NADH ratio was assessed using the NAD+/NADH Assay Kit (ab65348). Initially, cells were digested in 120 µL of NADH/NAD extraction buffer. After centrifugation in a 10 kD Spin Column (ab93349) at 14,000 x g for 20 minutes at 4°C, half of the sample was transferred to a new tube and incubated at 60°C for 30 minutes to decompose NAD+, while the remaining half was designated as NADt (comprising both NADH and NAD+). Subsequently, 20

μL of NADt and 20 μL of the decomposed NAD+ sample were mixed with 30 μL of extraction buffer and then incubated with 100 μL of reaction mix at room temperature for 5 minutes, facilitating the conversion of NAD+ to NADH. Following this, 10 μL of NADH Developer was added to each well, and the mixture was allowed to react at room temperature for 20 minutes. The resulting sample outputs were measured at OD 450 nm on a microplate reader (SpectraMax i3x Multi-Mode Microplate Reader) in kinetic mode.

Measurement of ATP Concentration

ATP concentration of the cells was determined by ATP Assay Kit (ab83355) according to the manufacturer's protocol. Cells were seeded at 1×10^6 cells/mL. The cells were collected and lysed in 150 μL of ATP assay buffer. Then, the samples were centrifuged for 5 min at 4 °C at 13,000× *g* to remove insoluble material and loaded to a 96-well plate (ThermoFisher Scientific) at a volume of 50 μL in 3 technical replies. The plate was incubated at room temperature for 30 min and protected from light. The absorbance was measured at wavelength $\lambda = 570$ nm by the spectrophotometer (SpectraMax i3x Multi-Mode Microplate Reader). The experiment was conducted using four biological replications and the collected data were calculated according to the producer's instructions. The data were presented as an ATP concentration (nmol) per 1 mg of total protein in each well.

Mitochondrial Membrane Potential

For the analysis of mitochondrial membrane potential (MMP), cells were subjected to JC-1 working solution (10 μg/ml) and subsequently incubated in a 5% CO2 incubator at 37 °C for a duration of 30 minutes. Following this incubation period, the JC-1-treated cells underwent three washes with PBS, with each wash lasting 2 minutes. Images were then acquired using a fluorescence microscope (Revolve, Echo, San Diego, California, USA). Carbonyl Cyanide

Chlorophenylhydrazone (CCCP, 50uM for 24h)

Mitochondrial ROS Production

a. MitoSOX-based flow cytometric assay

To evaluate mitochondrial ROS levels, we employed a MitoSOX-based flow cytometric assay on both control cells and cells subjected to antimycin A treatment (20uM for 30 minutes). Initially, primary VSMC from PGRN+/+ and PGRN-/- or aSMC and aSMC^{PGRN} were seeded in six-well plates and subsequently exposed to MitoSOX (5 μM) staining in complete medium for a half-hour at 37 °C. After staining, a gentle wash followed by 5-minute trypsinization at 37 °C was performed. Subsequently, the cells were resuspended in FACS buffer (comprising PBS, 1% BSA, and 1 mM EDTA) and subjected to immediate analysis via flow cytometry. The flow cytometer recorded both mean fluorescence intensity and the percentage of stained cells. The data were presented as histograms representing the cell count emitting specific fluorescence, effectively illustrating the size of the corresponding cell population. Graphs were generated to depict the mean fluorescence intensity, offering a quantifiable representation of the observed results. Additionally, the effects of antimycin A were presented by delta (difference between before and after drug incubation) in primary and cells overexpressing PGRN.

b. Lucigenin chemiluminescence assay

The chemiluminescent probe lucigenin (bis-N-methylacridinium nitrate) was used to assess ROS levels within the cells. A cell suspension, comprising up to 1 × 10^6 cells in 1 ml of Complete Phosphate-Buffered Saline (CPBS), was supplemented with 175 μL of lucigenin (0.005 mmol/L) and assay buffer. This mixture was then meticulously transferred to a White 96-well microplate. Subsequently, the microplate was promptly inserted into a

luminometer (FlexSation 3 microplate reader, Molecular Devices, San Jose, USA) to record the chemiluminescent response. These measurements were conducted at a constant temperature of 37°C and spanned a duration of 60 minutes. Following the initial reading, NADPH (0.1 mmol/L), serving as a substrate for the NADPH oxidase enzyme, was introduced to the suspension. A second reading of the microplate was subsequently conducted. The results were expressed as relative light units (RLU) per protein levels. To confirm the mitochondrial origin of the ROS signal, VSMCs samples underwent incubation with antimycin A for 1 hour.

Extraction and Quantification of Mitochondrial DNA Content and Mitochondrial Biogenesis

Relative mtDNA copy numbers were estimated by real-time quantitative PCR according to previously described methods[169, 170]. Total DNA was isolated from cells adherent cultures by Genomic Mini Kit (Qiagen Dneasy blood & tissue kit) according to the producer's instructions. DNA probes were diluted in Rnase-free H_2O (Sigma-Aldrich), to equal concentration and stored at −20 °C until further use. The Mitochondrial DNA (mtDNA) content was assessed by absolute quantification of DNA copy numbers using real time PCR. mtDNA content analysis was performed with TaqMan Master Mix (Applied Biosystems) on Applied Biosystems® 7500 Real-Time PCR System (Life Technologies). mtDNA was detected using primers MT16520F and MT35R, in the presence of probe MT16557TM. Nuclear DNA content was estimated by amplification of a fragment from the single-copy gene Kir4.1, with primers KIR835F and KIR903R used together with probe KIR857TM. The results were calculated as mtDNA/nDNA content based on the ΔΔCt method according to the previously described method[171]. Peroxisome proliferator-activated receptor-γ coactivator-1α (PGC-1α), a transcription factor controlling many aspects of oxidative metabolism including biogenesis[172], was analyzed via western blot.

Mitochondrial Morphology and Dynamics

Via western blot, we measured Mitofusin 1 (Mfn1) and Optic Atrophy 1 (OPA1) as markers of mitochondria fusion, and Dynamin-Related Protein 1 (Drp1) as a marker of mitochondria fission.

Mitophagy Study

To investigate mitophagy within cells, we conducted a comprehensive examination of protein expression using western blot analysis. Specifically, we assessed the levels of key markers involved in mitophagy, including LC3A, p62, PINK1, and PARKIN. To investigate mitophagy in fresh aorta, we utilized a unique transgenic mouse known as the mt-Keima mouse, graciously provided by Dr. Finkel from the University of Pittsburgh. This model is characterized by the expression of mt-Keima, a pH-dependent fluorescent protein, within the mitochondria. Mt-Keima, a coral-derived protein, is a dual-excitation radiometric fluorescent protein known for its pH sensitivity and resilience against lysosomal proteases. In the mitochondria's physiological pH environment (pH 8.0), it predominantly emits shorter-wavelength excitation, rendering a green appearance. However, during mitophagy within the acidic lysosome (pH 4.5), mt-Keima progressively transitions towards longer-wavelength excitation, resulting in a red fluorescence emission[173]. Following the dissection of aortae from mt-Keima mice, they were divided into control and mt-Keima-treated groups after incubation with LV for 24 hours. Subsequently, the aortae were longitudinally opened and had their endothelium removed before being mounted on glass slides and covered with coverslips. Images were acquired using a fluorescence microscope (Revolve, Echo, San Diego, California, USA).

2.2.17 Lysosome Biogenesis

In whole cell lysate, we studied lysosome biogenesis by measuring lysosomal-associated membrane protein (LAMP1) expression and the phosphorylation status of transcription factor EB (TFEB). In cytoplasm and nuclear fractions, we evaluated the TFEB content via western blot analysis. Fractioning was performed as described below.

2.2.18 Cytoplasm and Nuclear Fractions Preparation

Nuclear protein extracts were prepared using a nuclear extraction kit (Thermo Fisher, #78833) following the manufacturer's guidelines. The quantification of total TFEB in cytoplasm and nuclear fractions was conducted through western blotting. For cytoplasmic fractions, GAPDH expression served as an internal control for the cytoplasm fraction, while histone3 was used as an internal control for the nuclear fractions.

2.2.19 Statistical Analysis

The calculation of the maximal effect (Emax) from KCl, PE, and TXA2 were conducted through the analysis of CRC. pD2 resulting from CRCs was also calculated. CRCs were fitted using a non-linear interactive fitting program (Graph Pad Prism 9.0; GraphPad Software Inc., San Diego, CA, USA). The term "Emax" means the highest attainable effect produced by KCl, PE, and TXA2. While "pD2" indicates the negative logarithm of the molar concentration of phenylephrine and thromboxane needed to activate 50% of the maximum effect (EC50).

For comparisons of multiple groups, one-way or two-way analysis of variance (ANOVA),

followed by the Tukey post-test was used. Differences between the two groups were determined using Student's t-test. The vascular function data are expressed as a maximal response. The concentration–response curves were fitted by nonlinear regression analysis. Maximal response was determined and used to determine if there was difference between the groups. Analyses were performed using Prism 10.0 (GraphPad Software, La Jolla, CA). A difference was considered statistically significant when $P \leq 0.05$.

2.3 Results

2.3.1 Deficiency in PGRN Affects Vascular Contractility *ex vivo*

To analyze whether PGRN regulates vascular contraction, we examined the effects of KCl (120mM), phenylephrine, or thromboxane A2 analogue (U46619) in endothelium-denuded aortic rings from PGRN+/+ and PGRN-/- mice via wire myograph. Deficiency in PGRN decreased the vascular contractu7ntutility to all three agents in male (Fig. 1B-D) and female mice (Fig. 1E-G) and diminished the protein but not mRNA for αSMA level (Fig. 1H and I). In addition, lack of PGRN did not affect the vascular thickness at least in mice with 12-14 weeks of age (Fig. 1J).

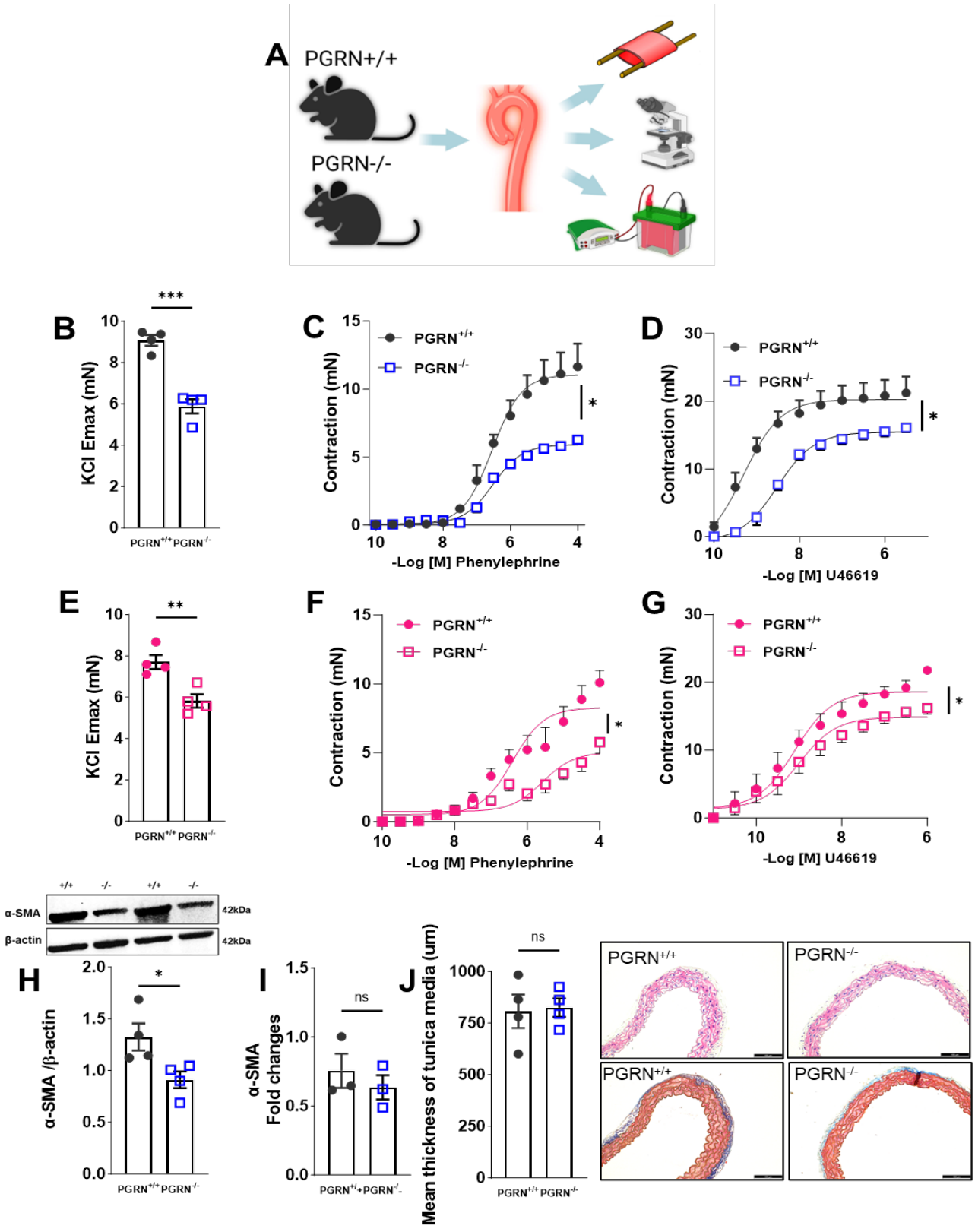

Figure 1. Deficiency in PGRN Impairs Vascular Contractility *ex vivo*

(A) Schematic Representation of the *Ex Vivo* Mouse Experiment Setup. This schematic illustrates the experimental setup for ex vivo experiments involving thoracic aortas isolated from PGRN+/+ and PGRN-/- mice. The aortas were utilized for wire myography, western blot analysis, quantitative PCR (qPCR), and Hematoxylin and Eosin (H&E) staining.(B-D) *Ex vivo* wire myography showing KCl-induced vascular contractility (120mM) (B), and concentration-effect curves to phenylephrine (C), and thromboxane A2 analogue (U46619) (D) in aortae from PGRN-/- and PGRN+/+ mice in endothelium-denuded aortic rings in Male mice. (E-G) *Ex vivo* wire myography showing KCl-induced vascular contractility (120mM) (E), and concentration-effect curves to phenylephrine (F), and thromboxane A2 analogue (U46619) (G) in aortae from PGRN-/- and PGRN+/+ mice in endothelium-denuded aortic rings in Female mice (H) Western blot for protein expression of αSMA in PGRN-/- mice compared to PGRN+/+ mice aorta. β-actin was used as load control. (I) mRNA expression of αSMA gene in PGRN-/- and PGRN+/+ mice aorta measured by qPCR. (J) Images of Hematoxylin & eosin and Masson's trichrome stains in thoracic aortae. Scale bar, 100 µm. Morphometric analysis of media area in PGRN-/- and PGRN+/+ mice aged 12-14 weeks. Data are presented as mean ± SEM (n = 3-7). *P < 0.05 vs. PGRN+/+ mice

2.3.2 Deficiency in PGRN Induces Inflammation *ex vivo*

Deficiency in PGRN triggered vascular inflammation in male and female mice characterized by a substantial increase in the expression of inflammatory genes such as ICAM, VCAM, IL1β and increased expression of pro-inflammatory cytokines such as TNFα, and IL6 genes in PGRN+/+ and PGRN-/- mice (Fig. 2A and B).

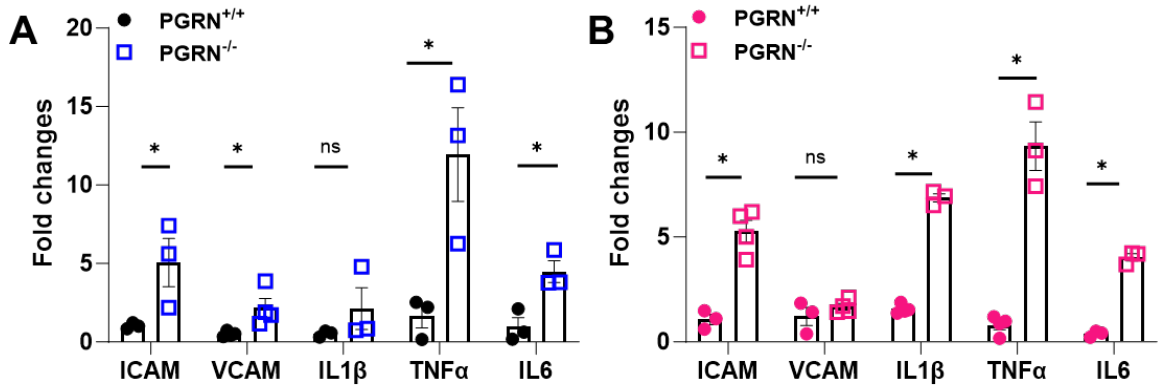

Figure 2. PGRN Deficiency Induces Inflammation *ex vivo*

(A-B) mRNA expression of inflammatory marker genes in PGRN+/+ and PGRN-/- male (A) and female (B) mice aorta by RT-PCR. Data are presented as mean ± SEM (n = 3-7). *P < 0.05 vs. PGRN+/+ mice

2.3.3 Deficiency in PGRN Affects Vascular Cell Contractility *in vitro*

We further examined the role of PGRN regulating vascular contraction in primary aVSMC isolated from PGRN+/+ and PGRN-/- (Fig. 3A). By performing the collagen gel disc assay, we observed that PGRN-/- aVSMC contracted less after 48h compared to PGRN+/+ aVSMC (Fig. 3B). Furthermore, we found attenuated F-actin and αSMA levels (Fig. 3C-D), with no difference in αSMA mRNA expression (Fig. 3E).

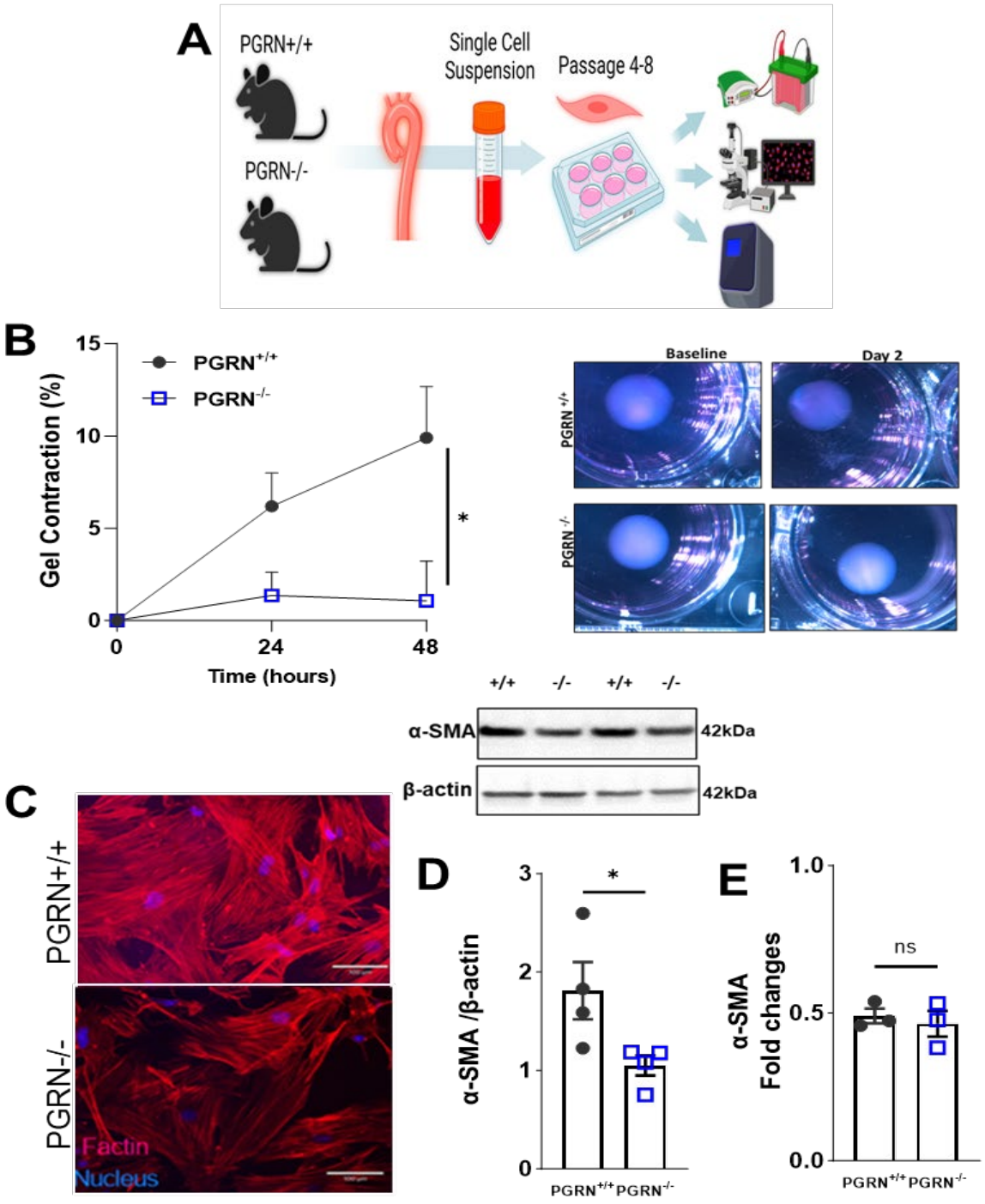

Figure 3. PGRN Deficiency Induces Loss of VSMC Contractility *in vitro*

(A) Schematic Representation of *In Vitro* Experiment Setup. This schematic diagram illustrates the setup for in vitro experiments involving primary aVSMCs isolated from the thoracic aorta of both PGRN+/+ and PGRN-/- mice. These isolated aVSMCs were employed in gel contraction studies, Western blot analysis, quantitative PCR (qPCR), and phalloidin staining. (B) Collagen contraction assay in PGRN+/+ and PGRN-/- aVSMC. Gel area variation on day 2 post-gelation normalized to baseline area. Scale bar, 1 mm. Measurement of diameter over time. (C) Representative image of of actin filaments in PGRN+/+ and PGRN-/- aVSMC. In red, actin filaments stained with Rhodamine-

Phalloidin; in blue, nuclei stained with DAPI. Scale bar, 100 μm. (D) Western blot for protein expression of αSMA in PGRN+/+ and PGRN-/- aVSMC. β-actin was used as load control. (E) mRNA expression of αSMA gene measured by qPCR in PGRN+/+ and PGRN-/- aVSMC. Data are presented as mean ± SEM (n = 3-4). *P < 0.05 vs. PGRN+/+ aVSMC

2.3.4 PGRN is a Major Regulator of Mitochondrial Function *in vitro*

In diabetic nephropathy[63] or in neuroblastoma cells[174], PGRN seems to regulate mitochondria quality. Thus, we characterized if mitochondria profile in the vasculature are regulated by PGRN. In aVSMC, lack of PGRN attenuated Oxygen Consumption Rate (OCR) (Seahorse) followed by suppression of ATP levels, mitochondrial complex I activity, and NAD^+/NADH ratio (Fig. 4A-D).

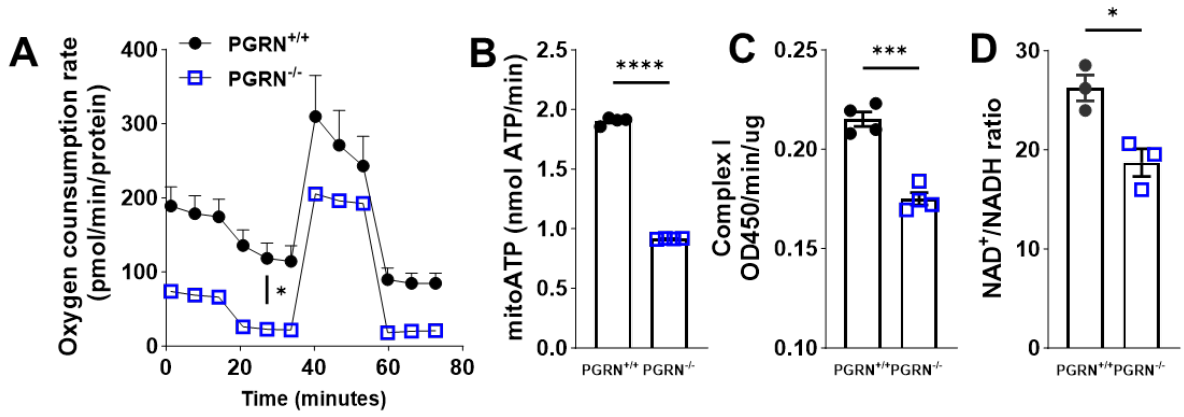

Figure 4. Loss of PGRN Affects Mitochondrial Function in aVSMCs

(A) Mitochondrial oxygen consumption rates (OCR) in PGRN+/+ and PGRN-/- aVSMCs measured using the Seahorse XF Extracellular Flux 96 analyzer. (B) ATP content quantified by colorimetric assay in PGRN+/+ and PGRN-/- aVSMCs. (C) OXPHOS complex I (CI) enzyme activity by colorimetric assay in PGRN+/+ and PGRN-/- aVSMCs. (D) The NAD+/NADH ratio measured by colorimetric assay in PGRN+/+ and PGRN-/- aVSMCs. Data are presented as mean ± SEM (n = 3-6). *P < 0.05 vs. PGRN+/+ aVSMC

2.3.5 PGRN is a Major Regulator of Mitochondria Mass *in vitro*

Interestingly, lack of PGRN did not affect the mitochondria number (mtDNA/nDNA) (Fig. 5A) but decreased PGC1α expression (a marker of mitochondria biogenesis) (Fig. 5B), thus suppression of PGC1α might not be affecting mitochondrial biogenesis, but other signaling instead including inflammation and antioxidant machinery[175, 176].Since we observed suppressed complex I activity, we analyzed the complexes expression by using the OXPHOS antibody, which revealed that deficiency in PGRN reduces complexes I and II expression (Fig. 5C).

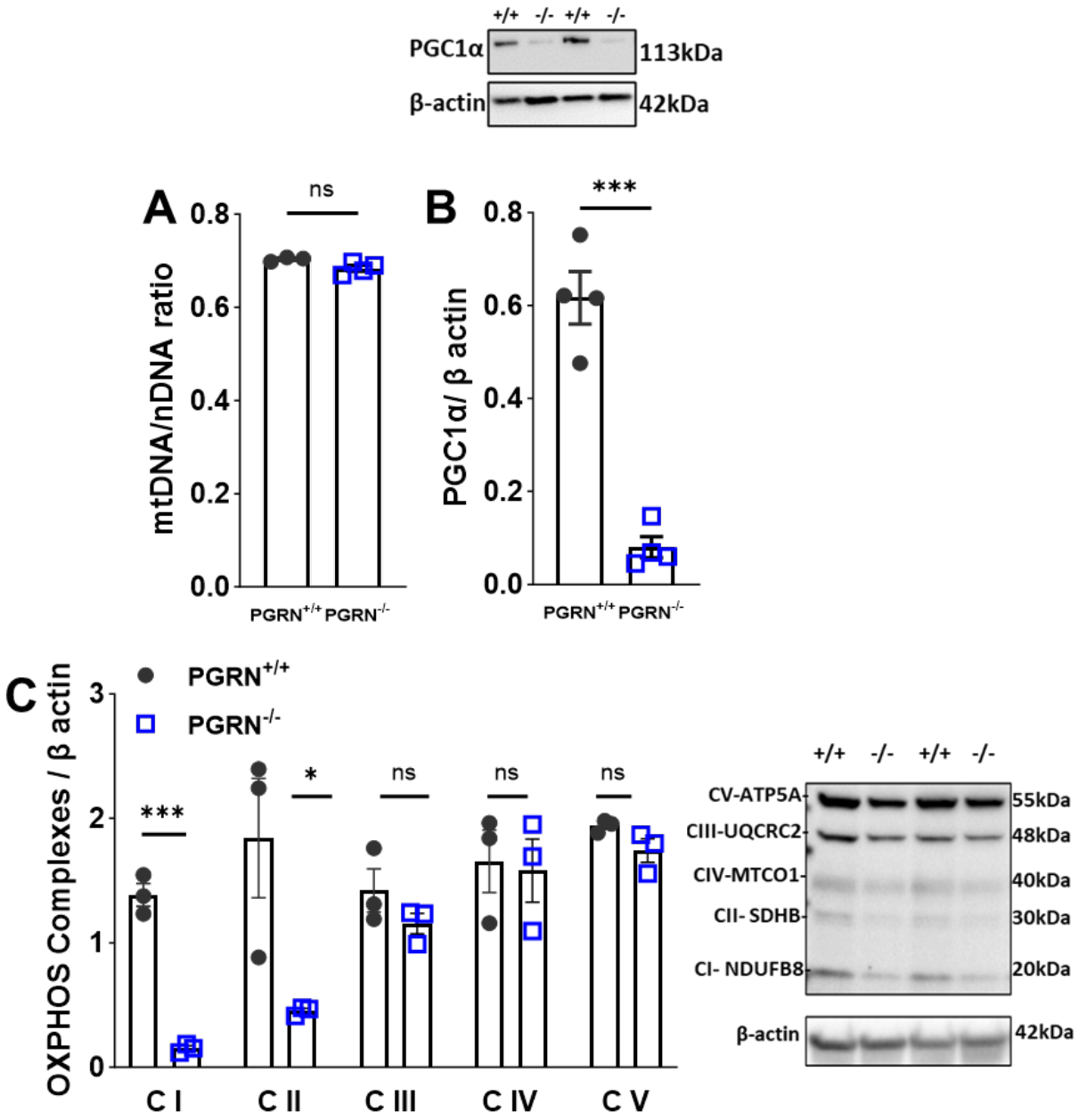

Figure 5. Loss of PGRN Reduces the Expression of PGC1α and Complexes I and II

(A) Quantitative PCR (qPCR) analysis of mitochondrial DNA (mtDNA) copy number relative to nuclear DNA (nuDNA) in PGRN+/+ and PGRN-/- aVSMCs. (B) Western blot for protein expression of PGC1α in PGRN+/+ and PGRN-/- aVSMCs. β-actin was used as load control. (C) Western blot for Protein expression of OXPHOS in PGRN+/+ and PGRN-/- aVSMCs. β-actin was used as load control. Data are presented as mean ± SEM (n = 3-6). *P < 0.05 vs. PGRN+/+ aVSMC

2.3.6 Loss of PGRN Affects Mitochondria Biogenesis and OXPHOS

Furthermore, aortae from PGRN+/+ and PGRN-/- displayed reduced complex I related genes, and peroxisome proliferator-activated receptor γ (PPARγ, a complex I gene regulator[177]) levels in males (Fig. 6A-B) and females (Fig. 6C-D) . In summary, PGRN deficiency reduce mitochondrial respiration primarily by reducing the expression of complex I and not by altering the mtDNA levels.

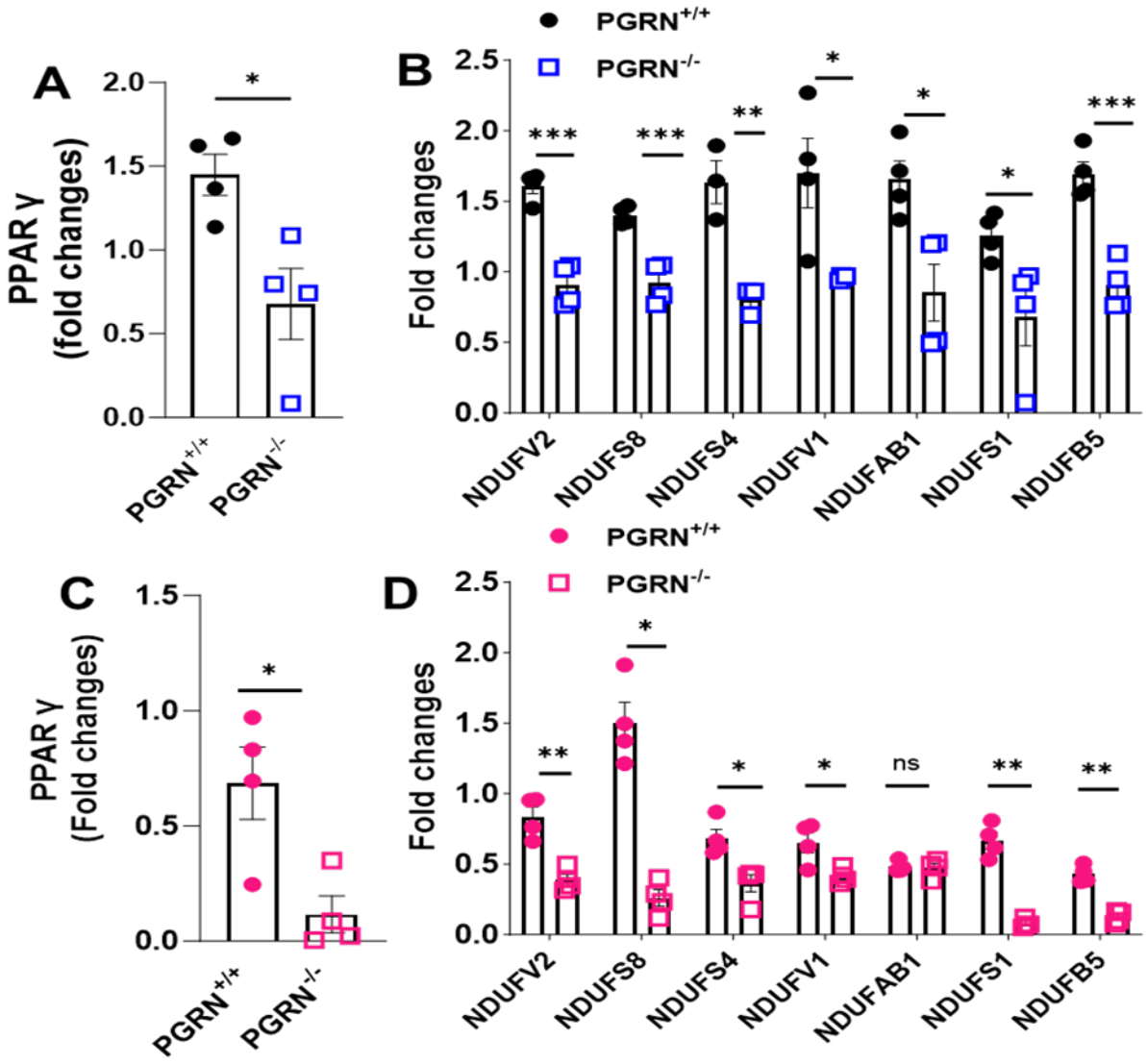

Figure 6. Loss of PGRN Affects Mitochondrial Biogenesis and OXPHOS

PPARϒ and expression of complex I genes in aortae from PGRN+/+ and PGRN-/- male (A-B) and female mice (C-D). Data are presented as Mean ± SEM. N=3-4. *P<0.05 vs PGRN+/+

2.3.7 Loss of PGRN Affects Markers of Mitochondrial Dynamics

Changes in mitochondria dynamic is crucial to maintaining mitochondria respiration, thus we studied if PGRN regulates markers of mitochondria fusion and fission. Lack in PGRN induced the expression of a marker of mitochondria fragmentation (fission) DRP1(Fig. 7A) and

downregulated MFN1 expression (marker of fusion) (Fig. 7B). Finally, mitochondria in PGRN-/- VSMC demonstrated impaired membrane potential, which was measured by JC-1 stain (Fig. 7C). Carbonyl Cyanide Chlorophenylhydrazone (CCCP) was used as a positive control in PGRN+/+ VSMC.

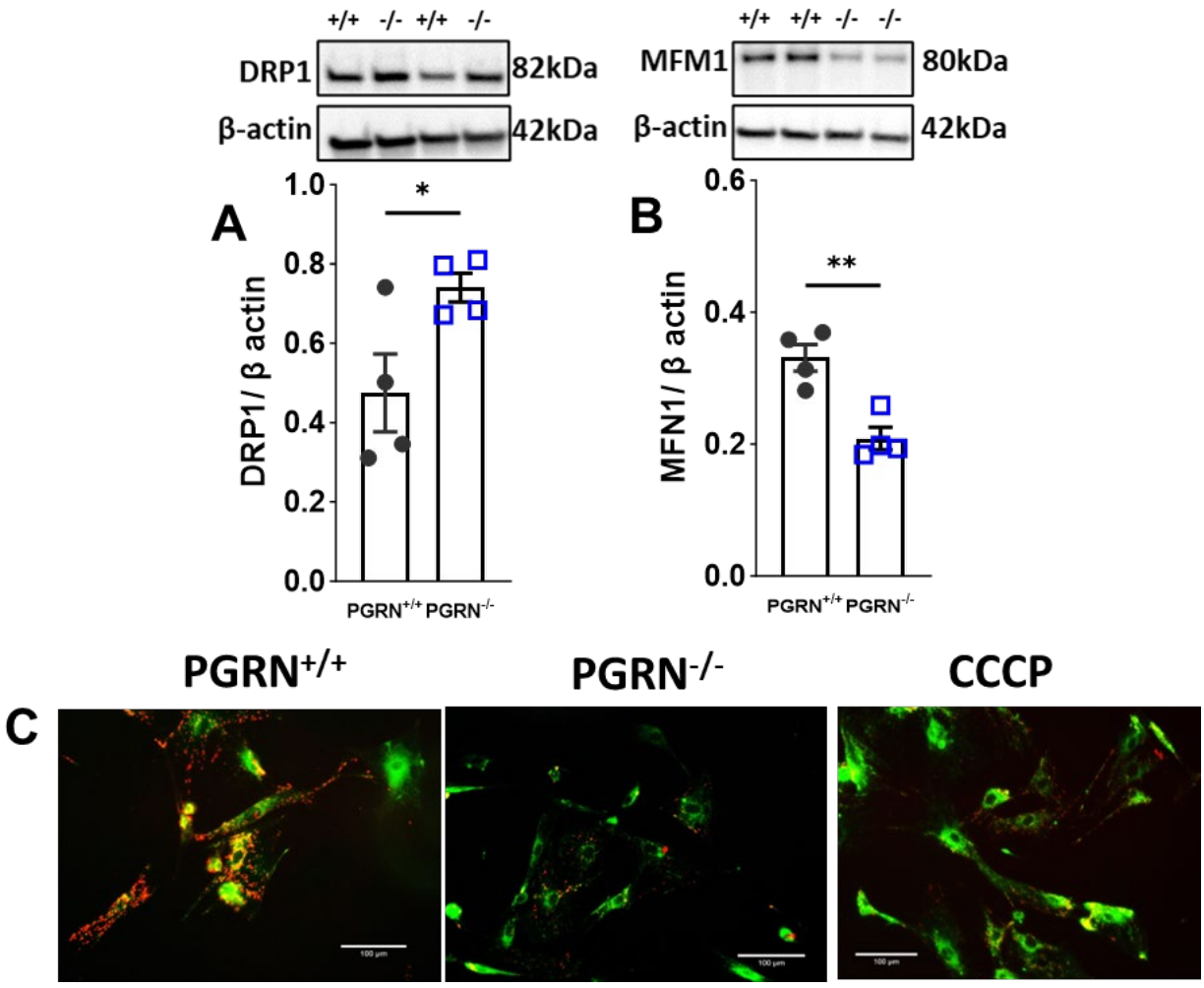

Figure 7. Loss of PGRN Affects Mitochondrial Dynamics and Membrane Potential in aVSMCs

(A) Western blot for protein expression of DRP1 in PGRN+/+ and PGRN-/- aVSMCs. β-actin was used as load control. (B) Western blot for protein expression of Mfn1 in PGRN+/+ and PGRN-/- aVSMCs. β-actin was used as load control (C) Mitochondria membrane potential, measured by JC-1 stain in PGRN-/- and PGRN+/+ aVSMCs. Normal mitochondrial membrane potential is shown in red.Depolarized membrane potential is shown in green. Carbonyl Cyanide Chlorophenylhydrazone (CCCP) was used as a positive control in PGRN+/+ VSMC. Data are presented as mean ± SEM (n = 3-6). *P < 0.05 vs. PGRN+/+ aVSMC

2.3.8 Loss of PGRN Produces Reactive Oxygen Species

Finally, changes in mitochondria respiration and dynamic have been associated with exacerbated mtROS formation. By using MitoSox we found that lack of PGRN induced mtROS formation (Fig. 8A), which is exacerbated by antimycin A (a potent mitochondrial ROS inducer) (Fig. 8B and C). Similar results were obtained by lucigenin chemiluminescence assay (Fig 8D). ERK1/2, a MAPK member and ROS-sensitive protein, was overactivated in PGRN-/- VSMC, but ERK1/2 activation in response to PDGF-BB was similar PGRN+/+ and PGRN-/0 VSMC (Figure 8E and F).

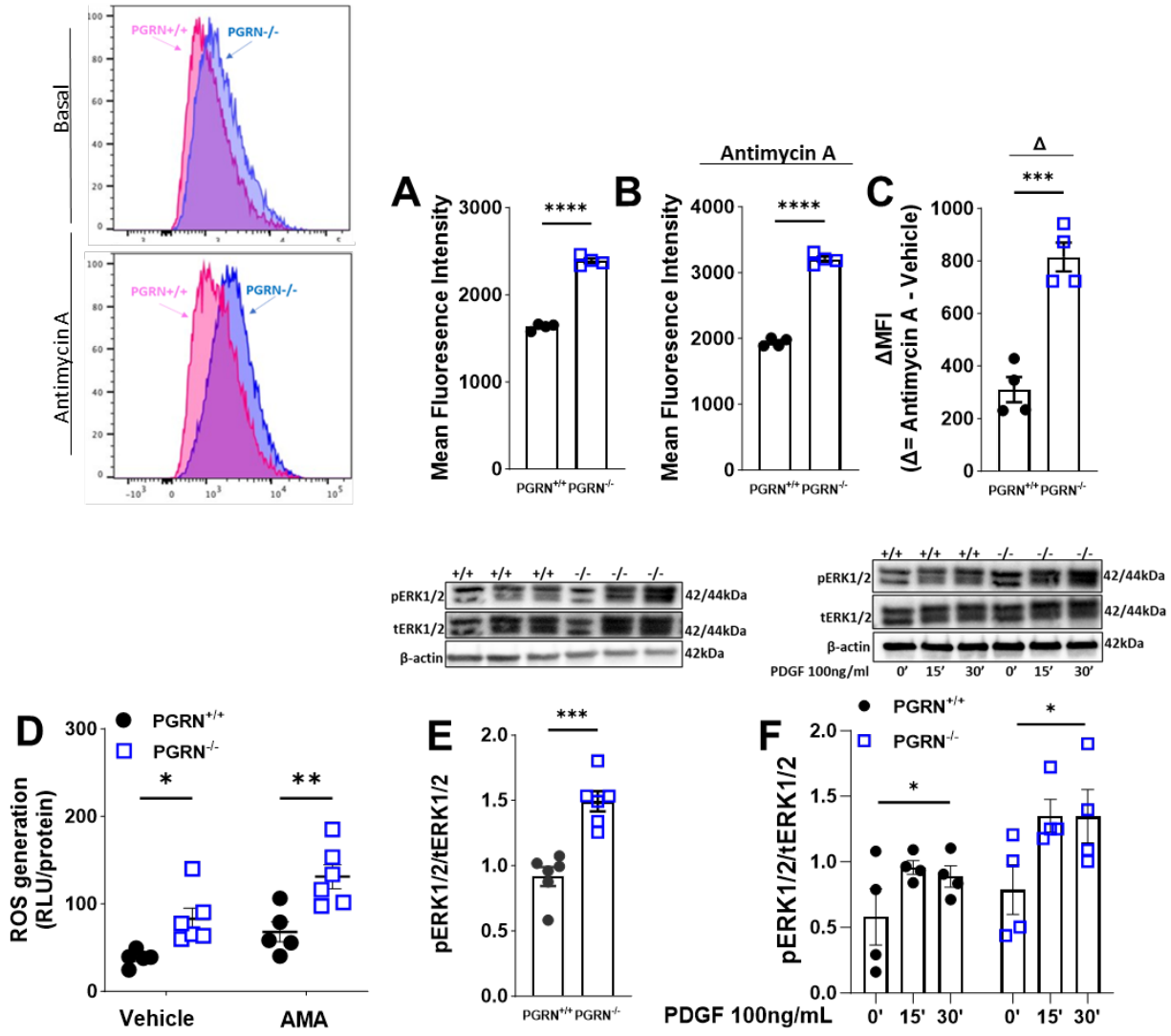

Figure 8. Loss of PGRN Affects Mitochondrial Reactive Oxygen Species (ROS) in aVSMCs

(A) Mitochondrial reactive oxygen species (mtROS) levels measured by flow cytometry in PGRN+/+ and PGRN-/- aVSMCs. MFI: Mean fluorescence intensity. (B) Mitochondrial reactive oxygen species (mtROS) levels measured by flow cytometry in PGRN+/+ and PGRN-/- aVSMCs treated with Antimycin A. MFI: Mean fluorescence intensity. (C) Sensitivity of Antimycin A-induced Mitochondrial reactive oxygen species (mtROS) formation in PGRN+/+ and PGRN-/- aVSMCs. (D) Lucigenin chemiluminescence assay in PGRN+/+ and PGRN-/- aVSMCs. (E) Western blot for protein expression of ERK1/2 in PGRN+/+ and PGRN-/- aVSMCs. β-actin was used as load control. (F) Western blot for protein expression of ERK1/2 in PGRN+/+ and PGRN-/- aVSMCs in presence of PDGF (100ng/ml). β-actin was used as load control. Data are presented as mean ± SEM (n = 3-6). *P < 0.05 vs. PGRN+/+ aVSMC

2.3.9 PGRN is a Major Regulator of Mitochondria Quality in Fresh Aortae

We also evaluated whether changes in mitochondrial performance are observed in whole arteries (Fig. 9A). By utilizing Oroboros O2k respirometry we analyzed mitochondrial respiration in fresh aortae and found that mitochondrial complex I activity is impaired in PGRN-/- with no changes in complex II (coupled or uncoupled) (Fig. 9B). Furthermore, aortae from PGRN-/- displayed reduced complex I, III, and IV protein expression (Fig. 9C). And as observed in primary VSMC, aortae from PGRN-/- demonstrated reduced PGC1a and MFN1 expression and increased DRP1 (Fig. 9D-F).

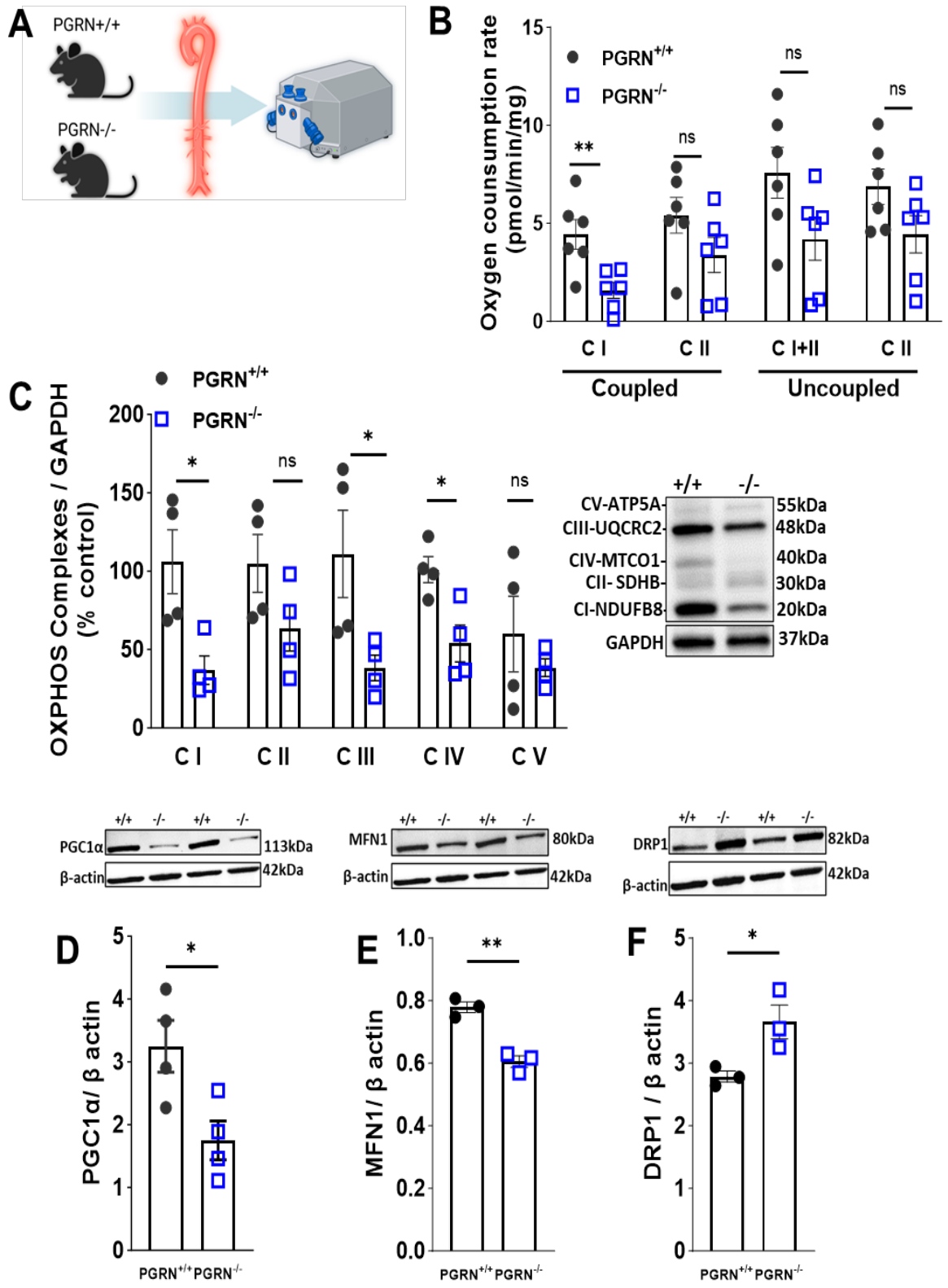

Figure 9. Loss of PGRN Affects Mitochondrial Quality in Fresh Aortae

(A) Mitochondrial oxygen consumption rates (OCR) in fresh aortae from PGRN+/+ and PGRN-/- measured using the Oroboros O2k respirometry. (B) Western blot for protein expression of OXPHOS. GAPDH was used as load control. (C-E) Western blot for protein expression of PGC1α, DRP1 and MFN1 levels. β-actin was used as load control. Data are presented as mean ± SEM (n = 3-4). *P < 0.05 vs. PGRN+/+ aVSMC

2.3.10 Effect of rPGRN on Mitochondrial Respiration and Vascular Contractility in PGRN-/- Arteries

Circulating PGRN plays a major role in regulating cardiovascular biology. Therefore, we treated PGRN-/- mice with rPGRN (20ug/day/mouse) for 7 days via osmotic mini-pump[139]; we found that PGRN treatment did not affect mitochondrial respiration in fresh aortae via Oroboros O2k respirometry(Fig. 10A).Similarly, rPGRN did not affect OCR in PGRN-/- VSMC measured by Seahorse analyzer (Fig. 10B)

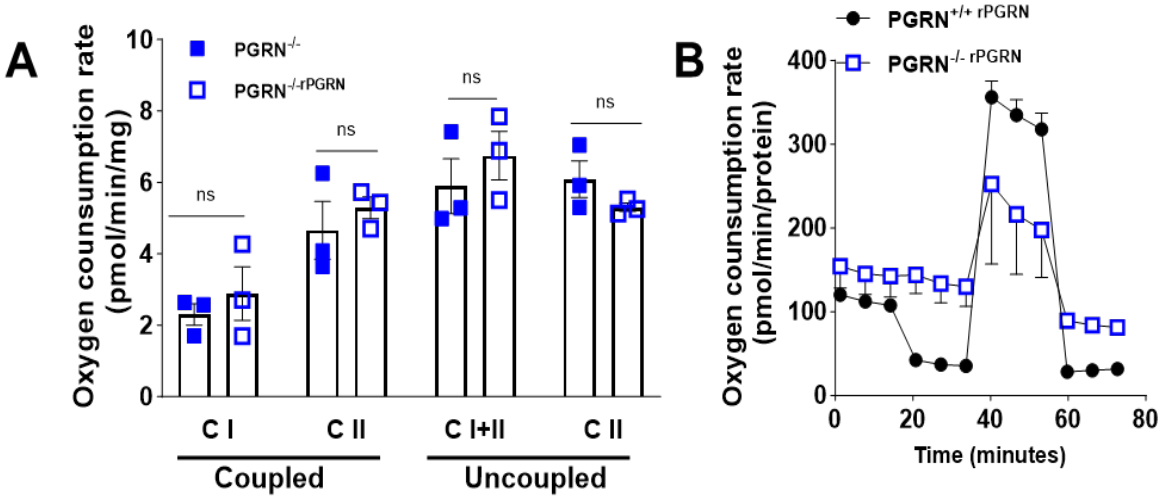

Figure 10. Circulating PGRN Does Not Alter Mitochondrial Respiration

(A) Mitochondrial oxygen consumption rates (OCR) analyzed via Oroboros O2k respirometry in aortae from PGRN-/- mice treated with rPGRN. (B) OCR measured by SeaHorse in VSMC from PGRN+/+ and PGRN-/- mice treated with rPGRN (600ng/mL, 24h). Data are presented as Mean ± SEM. N=3-4. *P<0.05 vs PGRN+/+ VSMC

2.3.11 Re-expression of PGRN Restores Mitochondrial Respiration and Vascular Contractility in PGRN-/- Arteries

Thus, we focused on understanding the intracellular role of PGRN by re-expressing PGRN via lentivirus delivery. We treated the aortae from PGRN+/+ and PGRN-/- with LV encoding PGRN for 24h and analyzed the mitochondrial respiration and vascular contractility (Figure 11A). LV increased PGRN expression in PGRN+/+ and repopulated PGRN in PGRN-/- (Figure 11B). In addition, LV increased complex I activity in Oroboros O2k respirometry (Figure 11C) but did not affect mitochondrial respiration in PGRN+/+ arteries (Figure 11D). LV treatment also improved vascular contractility to KCL, U46619, and phenylephrine in PGRN-/- arteries (Fig. 11E-G) but did not affect vascular contractility in PGRN+/+ arteries (Fig. 11H-J).

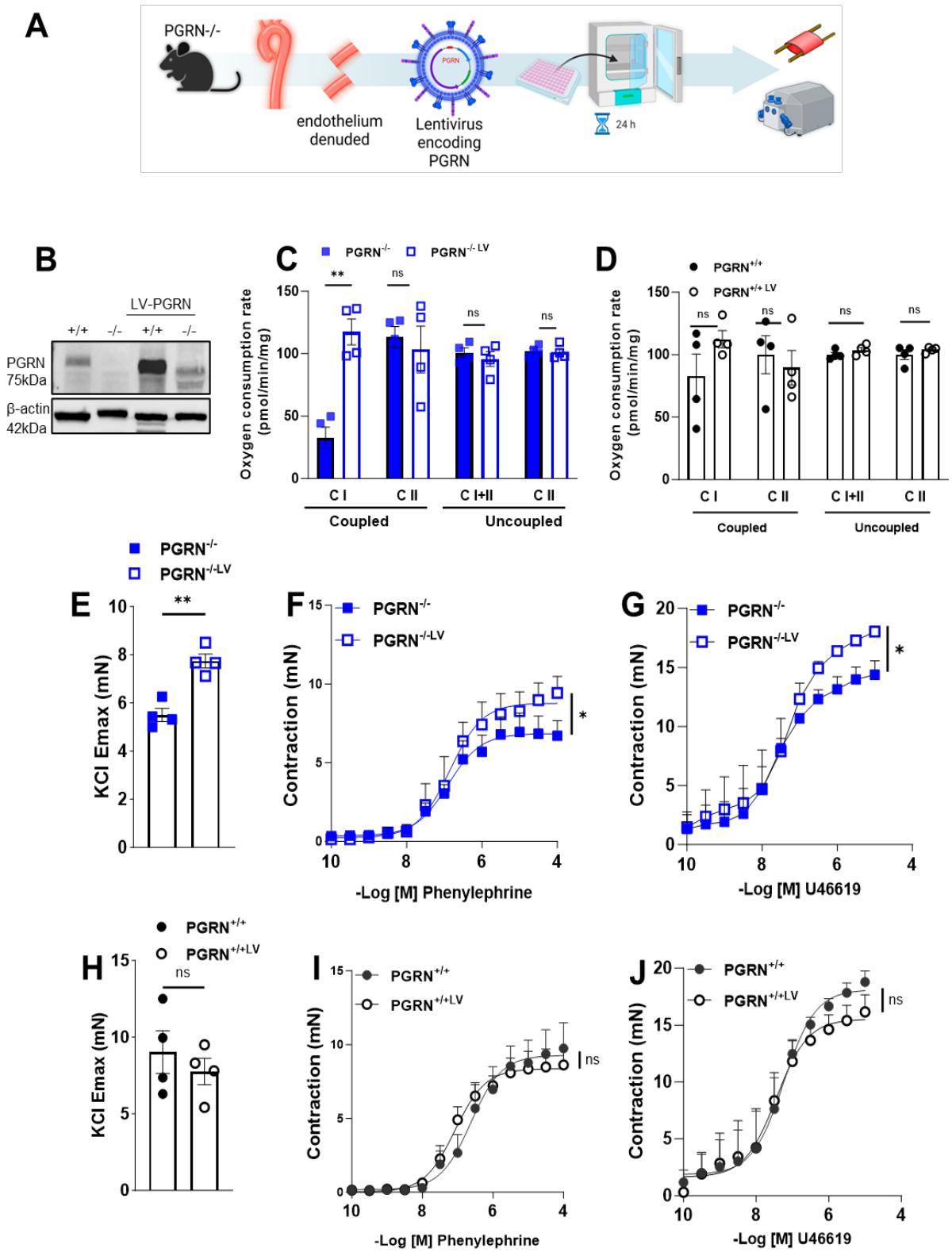

Figure 11. Re-Expression of PGRN Restores Mitochondrial Respiration and Vascular Contractility in PGRN Deficient Arteries

(A) Schematic Representation of *ex vivo* Experiment Setup. Circulating PGRN exerts significant regulatory effects on cardiovascular biology. To investigate the intracellular role of PGRN, we re-expressed PGRN using lentivirus delivery. PGRN+/+ and PGRN-/- aortae were treated with lentivirus encoding PGRN for 24 hours, followed by analysis of mitochondrial respiration and vascular contractility. (B) Western blot for protein expression of PGRN after LV treatment for 24hours. β-actin was used as load control. (C-D) Mitochondrial oxygen consumption rates (OCR) measured using the Oroboros O2k respirometry in fresh aortae from PGRN-/- mice (C) and PGRN+/+ mice (D) after LV treatment. (E-G) *Ex vivo* wire myography showing KCl-induced vascular contractility (120mM) (D), and concentration-effect curves to phenylephrine (E), and thromboxane A2 analogue (U46619) (F) in endothelium-denuded aortic rings of fresh aortae from PGRN-/- mice. (H-J) *Ex vivo* wire myography showing KCl-induced vascular contractility (120mM) (H), and concentration-effect curves to phenylephrine (I), and thromboxane A2 analogue (U46619) (J) after LV treatment in endothelium-denuded aortic rings of fresh aortae from PGRN+/+ mice. Data are presented as mean ± SEM (n = 3-4). *P < 0.05 vs. PGRN-/-

2.3.12 Effect of Over Expression of PGRN on Vascular Contractility and Mitochondrial Function in VSMCs

Since we found these exciting effects of LV-PGRN on regulating vascular contractility and mitochondrial respiration, we created VSMC overexpressing PGRN via LV delivery. PGRN expression was confirmed by western blot in cell lysate (Fig. 12A) and ELISA in the supernatant of aSMC (control) and $aSMC^{PGRN}$ (high expression of PGRN) (Fig. 12B). $aSMC^{PGRN}$ displayed higher cell contraction which could be observed in collagen gel disc assay and F-actin stain (more F-actin and smaller cell size) (Fig. 12C-D) and higher αSMA expression (Fig. 12E). $aSMC^{PGRN}$ demonstrated increased ATP levels, NAD^+/NADPH ratio, and complex I activity (Fig. 12F-H).

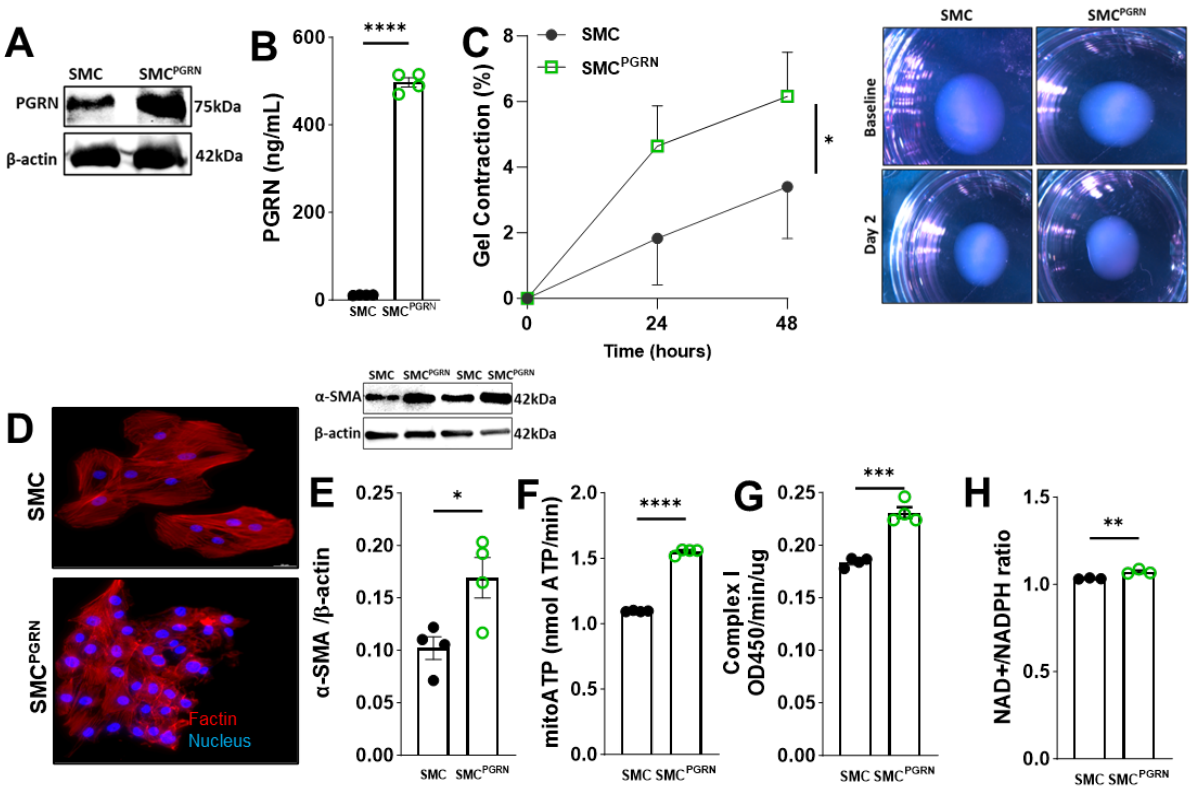

Figure 12. Overexpression of PGRN Induces Vascular Contractility in VSMC and Mitochondrial Function

(A) Western blot for protein expression of PGRN in SMC and SMC^{PGRN}. β-actin was used as load control. (B) Elisa for PGRN in supernatant of PGRN in SMC and SMC^{PGRN} (C) Collagen contraction assay in SMC and SMC^{PGRN}. Gel area variation on day 2 post-gelation normalized to baseline area. Scale bar, 1 mm. Measurement of diameter over time. (D) Representative image of actin filaments in SMC and SMC^{PGRN}. In red, actin filaments stained with Rhodamine-Phalloidin; in blue, nuclei stained with DAPI. Scale bar, 100 µm. (E) Western blot for protein expression of αSMA in SMC and SMC^{PGRN}. β-actin was used as load control. (F) ATP content quantified by colorimetric assay in SMC and SMC^{PGRN} . (G) OXPHOS complex I (CI) enzyme activity by colorimetric assay in SMC and SMC^{PGRN}.(H) The NAD+/NADH ratio measured by colorimetric assay in SMC and SMC^{PGRN}. Data are presented as mean ± SEM (n = 3-4). *P < 0.05 vs. SMC

2.3.13 Effect of Over Expression of PGRN on Markers of Mitochondrial Number, Biogenesis, and Dynamics in VSMCs

We examined the effects of aSMC^{PGRN} overexpression and found that it did not induce any significant changes in mitochondrial biogenesis or the overall mtDNA content within VSMCs (Fig. 13A and B). However, our investigation revealed an intriguing shift in markers of mitochondrial dynamics upon aSMC^{PGRN} overexpression. Specifically, we observed an increase in MFN1 expression but diminished DRP1 expression (Fig. 13C-D).

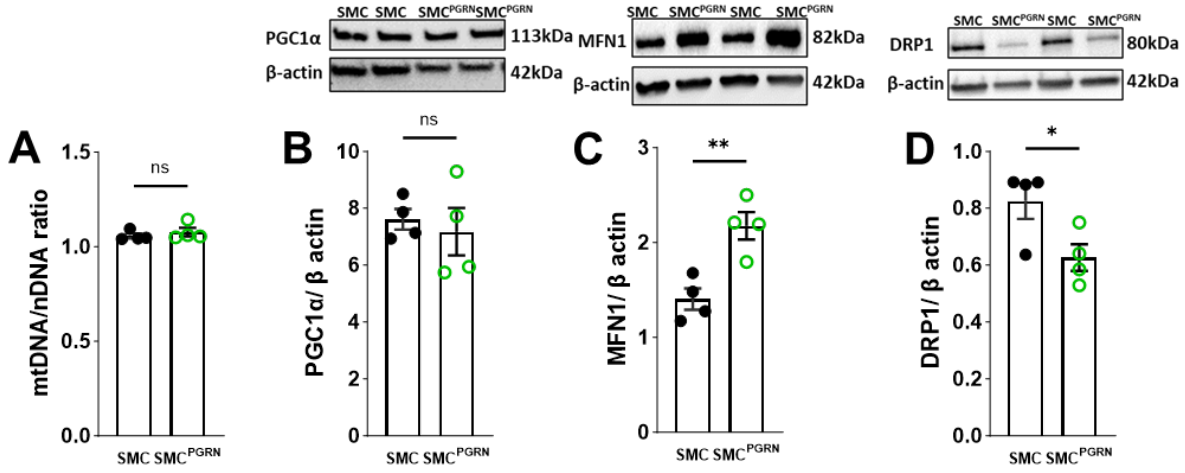

Figure 13. Overexpression of PGRN Affects Mitochondrial Number, Biogenesis and Dynamics

(A) Quantitative PCR (qPCR) analysis of mitochondrial DNA (mtDNA) copy number relative to nuclear DNA (nuDNA) in SMC and SMC^{PGRN} (B) Western blot for protein expression of PGC1α in SMC and SMC^{PGRN}. β-actin was used as load control. (C) Western blot for protein expression of MFN1 in SMC and SMC^{PGRN}. β-actin was used as load control. (D) Western blot for protein expression of DRP1 in SMC and SMC^{PGRN}. β-actin was used as load control. Data are presented as mean ± SEM (n = 3-4). *P < 0.05 vs. SMC

2.3.14 Effect of Over Expression of PGRN on Mitochondrial Reactive Oxygen Species (ROS) in VSMCs

As we previously examined ROS levels in PGRN+/+ and PGRN-/- VSMCs, we wanted to see the effect of overexpression of PGRN in cells. Our results revealed that the overexpression of PGRN in VSMCs had a notable impact on mtROS formation. Specifically, it resulted in a reduction in mtROS production. To further assess the protective potential of PGRN, we subjected the cells to antimycin A. Remarkably, the overexpression of PGRN not only reduced baseline mtROS but also provided protection against antimycin A-induced mtROS production (Fig. 14A-C).

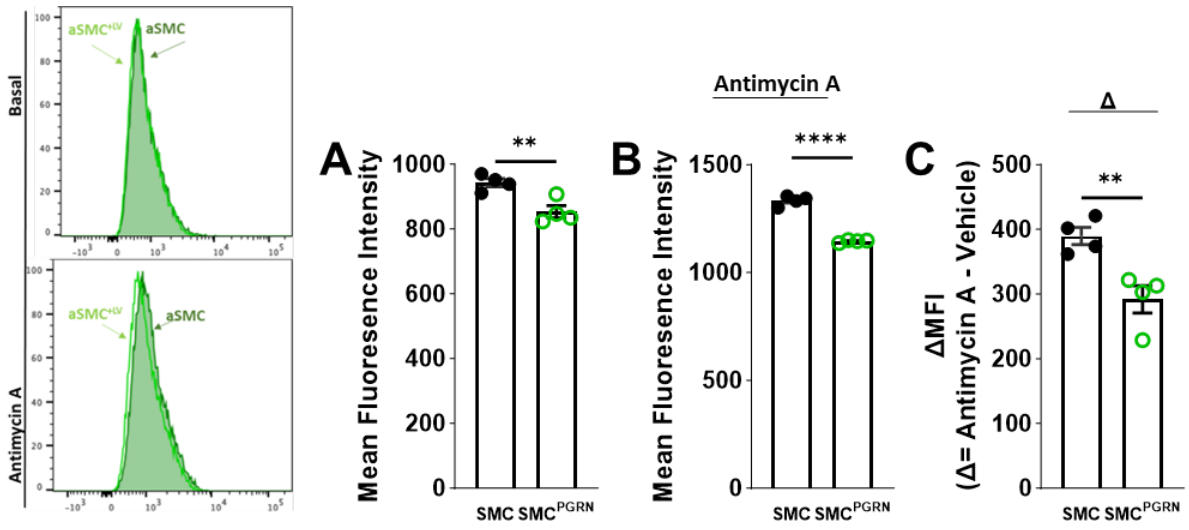

Figure 14. Overexpression of PGRN Affects Mitochondrial ROS Production

(A) Mitochondrial reactive oxygen species (mtROS) levels measured by flow cytometry in SMC and SMC^{PGRN}. MFI: Mean fluorescence intensity. (B) Mitochondrial reactive oxygen species (mtROS) levels measured by flow cytometry in SMC and SMC^{PGRN} treated with Antimycin A. MFI: Mean fluorescence intensity. (C) Sensitivity of Antimycin A-induced Mitochondrial reactive oxygen species (mtROS) formation in SMC and SMC^{PGRN}. Data were calculated by the delta between Antimycin A and vehicle effects. Data are presented as mean ± SEM (n = 3-4). *P < 0.05 vs. SMC

2.3.15 Deficiency in PGRN Disrupts Vascular Mitophagy and Lysosome Formation

Studies in kidneys have shown that PGRN regulates autophagy[63], but if PGRN affects vascular mitophagy is still unknown. Thus, we investigated whether disruption of PGRN signaling would affect mitochondrial recycling. We observed that VSMC from PGRN-/- present elevated PINK (66 and 33kDa), PARKIN, LC3I/II ratio, and p62 accumulation suggesting a dysfunctional mitophagy (Fig. 15A-D). Furthermore, we found an accumulation of LAMP1 (marker of lysosome), higher TFEB activity, characterized by higher TFEB content in the nuclei. (Fig. 15E and F). Suggesting that TFEB activation is higher in PGRN-/- VSMC, which leads to higher lysosome formation, however they are dysfunctional.

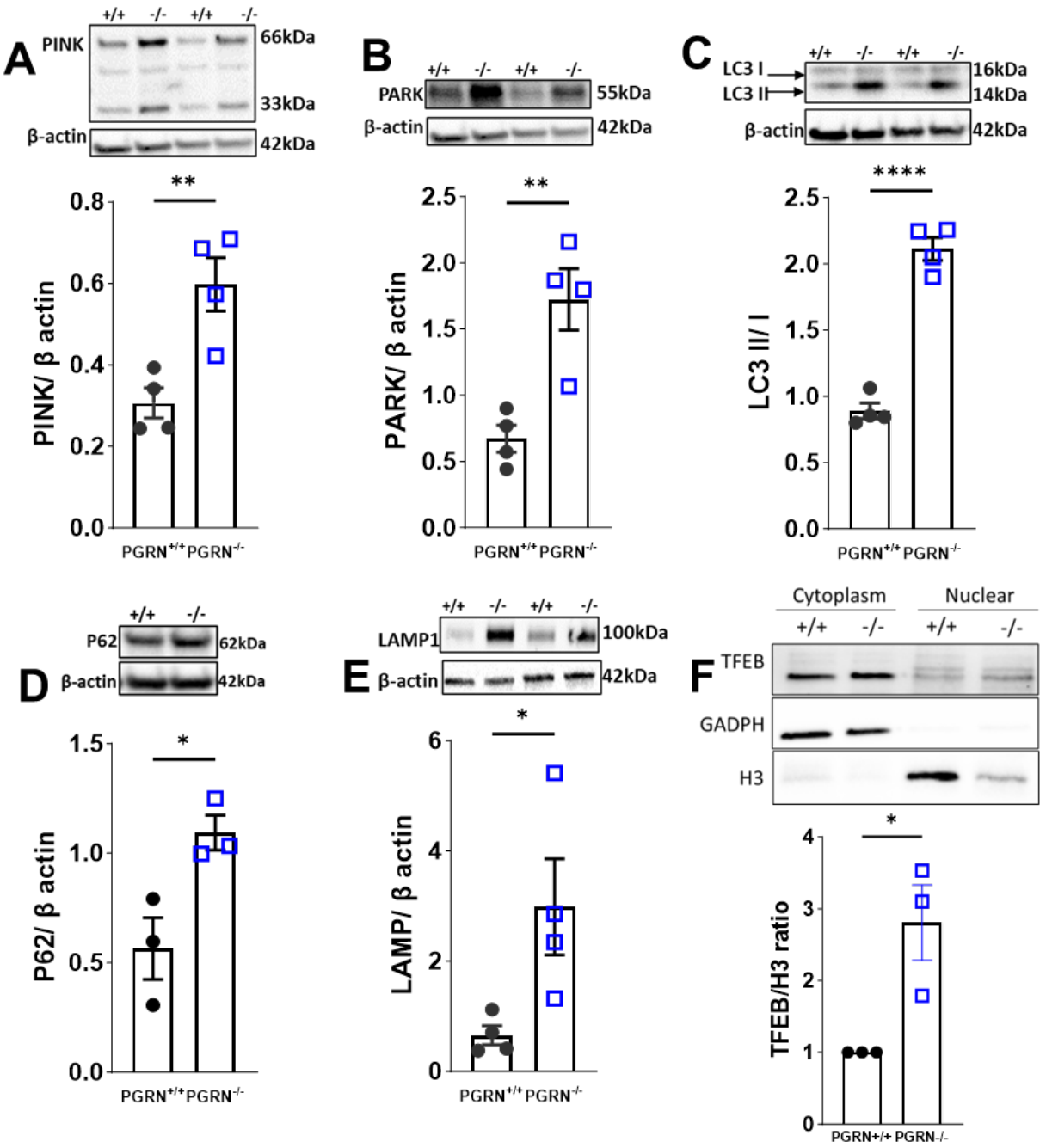

Figure 15. PGRN Deficiency Triggers Dysregulated Lysosome Formation and Disturbs Mitophagy Flux

(A-E) Western blot for protein expression of PINK (66 and 33 kDa) (A), PARK (B), LC3II/I (C) ratio, p62 (D), and LAMP1 (E) PGRN+/+ and PGRN-/- aVSMCs. β-actin was used as load control. (F) Western blot for TFEB of PGRN+/+ and PGRN-/- aVSMCs fractionated into cytoplasmic and nuclear samples. Protein expression quantification was normalized to GAPDH and Histone 3 (H3), a cytoplasm and nuclear markers, respectively. Data are presented as mean ± SEM (n = 3-4). *P < 0.05 vs. PGRN+/+

2.3.16 Effect of over Expression of PGRN on Vascular Mitophagy and Lysosome Formation

In VSMC overexpressing PGRN we observed reduced PINK, LC3I/II, and p62, with no difference in PARK and LAMP (Fig. 16A-E). Furthermore, we used arteries from mt-Keima mice to track mitophagy in fresh aorta, thus we overexpressed PGRN via LV delivery (24h of incubation) in aortae from those mice and tracked mitochondria flux. PGRN caused a remarkable increase of mitochondria in lysosome (red) compared to control arteries c (Fig. 16F). To confirm that high levels of PGRN induce autophagy we treated the cells with bafilomycin A1 (vacuolar H+-ATPase Inhibitor) and observed that accumulation of LC3II/I (Fig. 16G and H) indicating that PGRN is an autophagy inducer. Finally, we found that overexpression of PGRN triggered higher presence of TFEB in the nuclei (Fig. 16I), which suggests that PGRN induces lysosome biogenesis and autophagy.

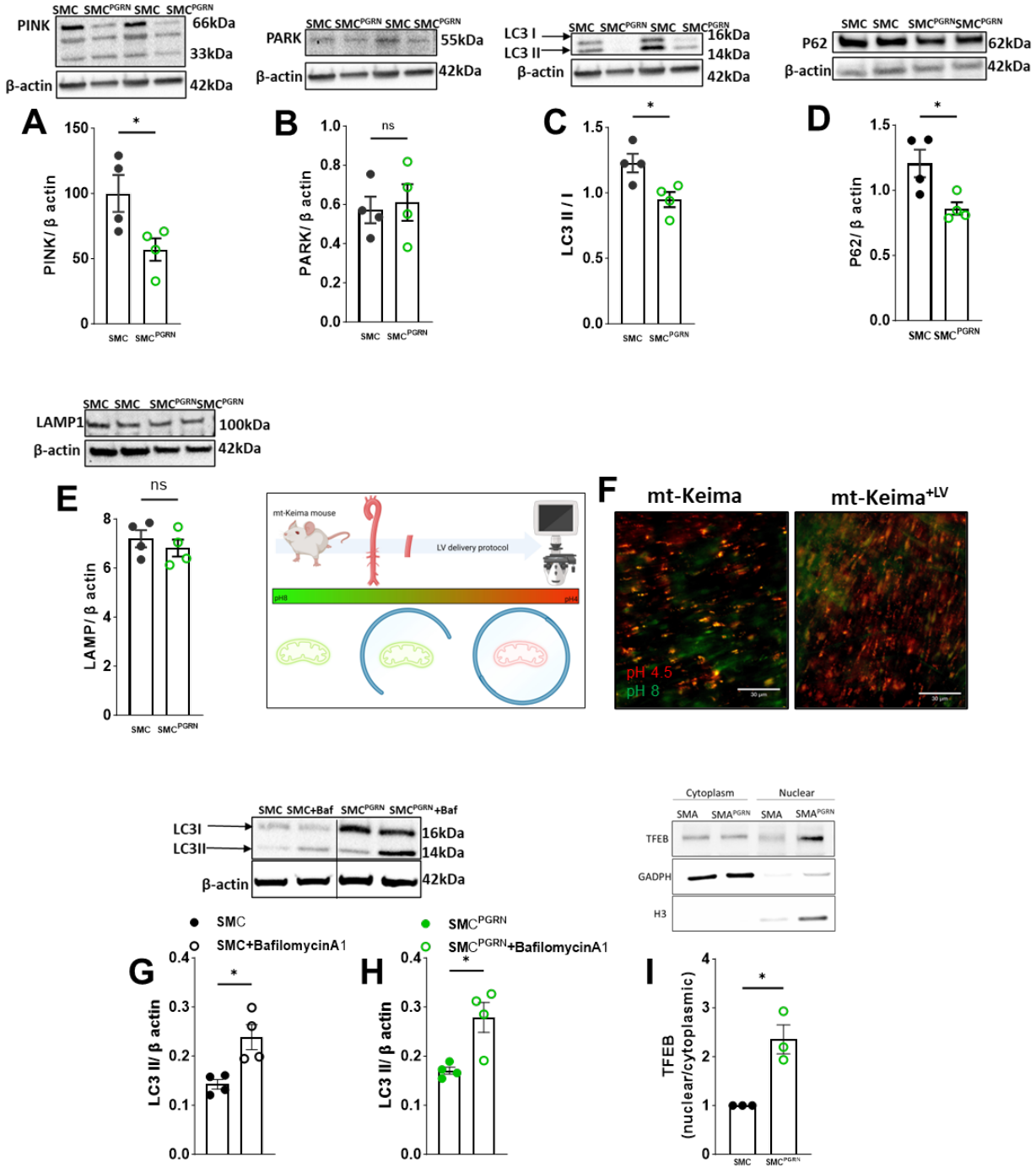

Figure 16. Overexpression of PGRN Confers an Accelerated Mitophagic Flux in VSMC

(A) Western blot for PINK (A), PARK (B), LC3AII/I (C), p62 (D) and LAMP (E) expression in SMC and SMC^{PGRN}. β-actin was used as load control. (F) Mitochondria flux in fresh aorta of mt-Keima enriched with PGRN via lentivirus delivery. Levels of green (located in the cytosol, basic pH) and red (located in the lysosome, acid pH) signals are shown as a function of cellular pH. Scale bar, 30um. (G-H) Western blot for LC3II/β-actin (G-H) in SMC and SMC^{PGRN} treated with bafilomycin A1. β-actin was used as load control. (P) Western blot for TFEB of SMC and SMC^{PGRN} fractionated into cytoplasmic and nuclear samples. Protein expression quantification was normalized to

GAPDH and Histone 3 (H3), a cytoplasm and nuclear markers, respectively. Data are presented as mean ± SEM (n=3-4). *P < 0.05 vs SMC; #P < 0.05 vs cell without treatment

2.3.17 Spermidine, an Autophagy Inducer, Rescues Mitochondrial Respiration and Vascular Contractility in PGRN Deficient Mice

We used spermidine as an autophagy inducer to analyze whether restoring autophagy flux would improve mitochondrial respiration and vascular contractility (Fig. 17A). To confirm that spermidine caused autophagy we measured LC3II/I in hearts from PGRN+/+ and PGRN-/- and observed that spermidine restored LC3A expression in PGRN-/- (Fig. 17B). Furthermore, spermidine increased the mitochondrial respiration in the aortae from PGRN-/- mice (Fig. 17C) but no change was observed in PGRN+/+mice (Fig. 17D). Spermidine treatment also increased vascular contractility in the aortae from PGRN-/- mice (Fig. 17E-G) but again we did not see any effect of spermidine in arteries from PGRN+/+ mice (Fig. 17H-J).

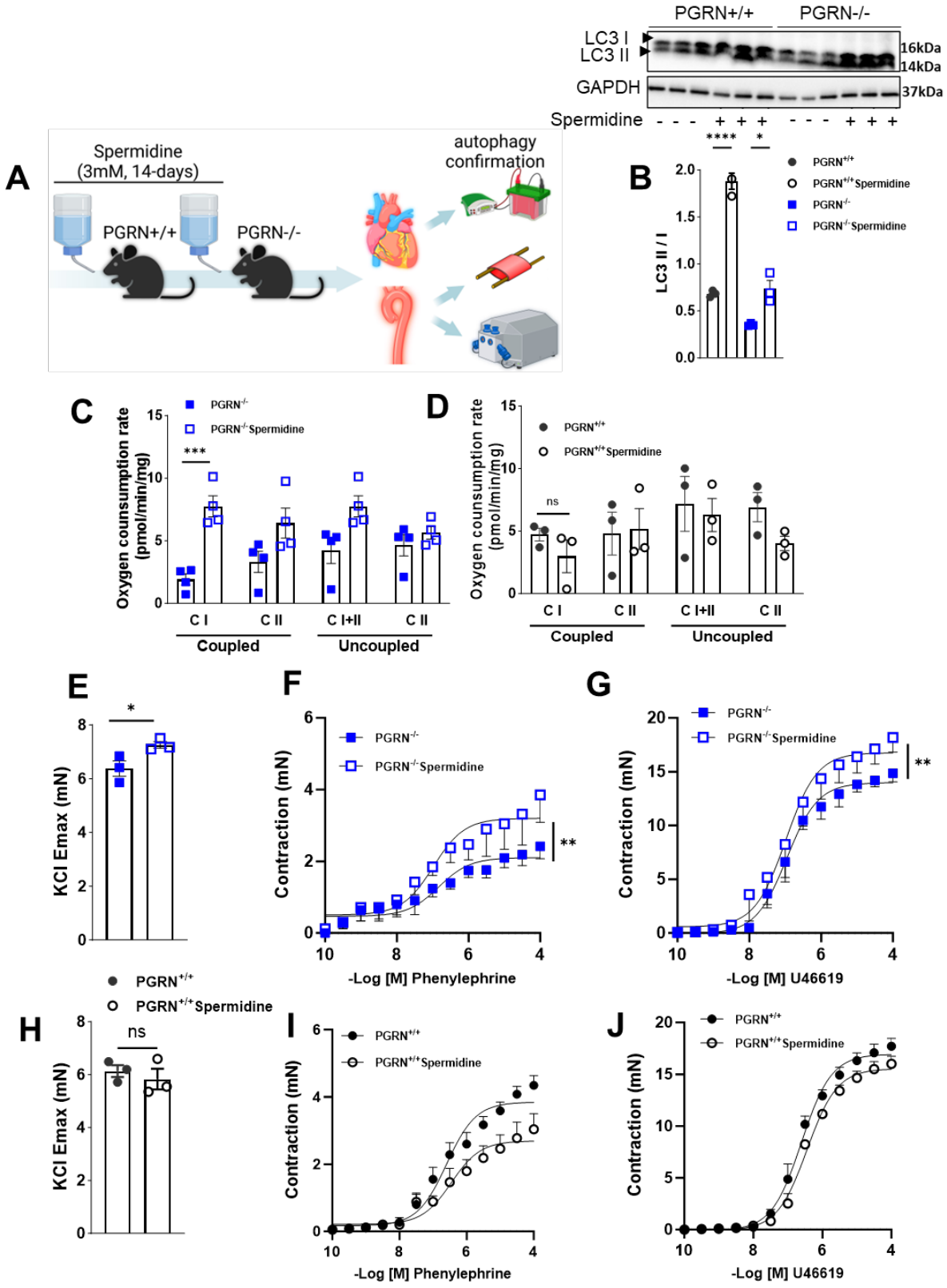

Figure 17. Spermidine, an Autophagy Inducer, Rescues Mitochondrial Respiration and Vascular Contractility

(A) Schematic Representation of *in vivo* Experiment Setup. We employed spermidine as an autophagy inducer in drinking water for 14 days, to assess whether reinstating autophagy flux could ameliorate mitochondrial respiration and vascular contractility. (B) Western blot for LC3AII/I expression in hearts from PGRN-/- mice treated or not with spermidine. GAPDH was used as load control. (C) Mitochondrial oxygen consumption rates (OCR) measured using the Oroboros O2k respirometry in fresh aortae from PGRN-/- mice treated or not with spermidine. (D-F) *Ex vivo* wire myography showing concentration-effect curves to KCl (120mM) (D), phenylephrine (E), and thromboxane A2 analogue (U46619) (F) in endothelium-denuded aortic rings of aortae from PGRN-/- mice treated or not with spermidine. (G) Mitochondrial oxygen consumption rates (OCR) measured using the Oroboros O2k respirometry in fresh aortae from PGRN+/+ mice treated or not with spermidine(H-J) *Ex vivo* wire myography showing concentration-effect curves to KCl (120mM) (H), phenylephrine (I), and thromboxane A2 analogue (U46619) (J) in endothelium-denuded aortic rings of aortae from PGRN+/+ mice treated or not with spermidine. Data are presented as mean ± SEM (n =4). *P < 0.05 vs PGRN-/- without treatment

2.3.18 Vascular Contractility in PGRN Deficient Mice not Normalized by Angiotensin II Treatment

We first analyzed whether Angiotensin II changes PGRN expression in aortae from PGRN+/+, which revealed that Angiotensin II upregulated PGRN protein expression (Fig.18A). We next challenged the PGRN+/+ and PGRN-/- mice with Angiotensin II (an inducer of vascular contraction and mitochondria dysfunction) to analyze mitochondria respiration and vascular function. We found that Angiotensin II did not change the mitochondria respiration in PGRN-/- compared to PGRN+/+ (the difference between PGRN+/+ and PGRN-/- persisted) (Fig.18B) and did not affect vascular contractility for phenylephrine and U46619 in PGRN-/- mice (Fig.18C-E), Finally, Angiotensin II similarly affected the vascular thickness in PGRN+/+ and PGRN-/-, but PGRN-/- were more sensitive to Angiotensin II-induced vascular fibrosis (Fig. 18F). These data suggest that Angiotensin II-induced vascular contractility relies on the integrity of PGRN signaling pathway, whereas PGRN seems to be a gatekeeper for fibrosis formation.

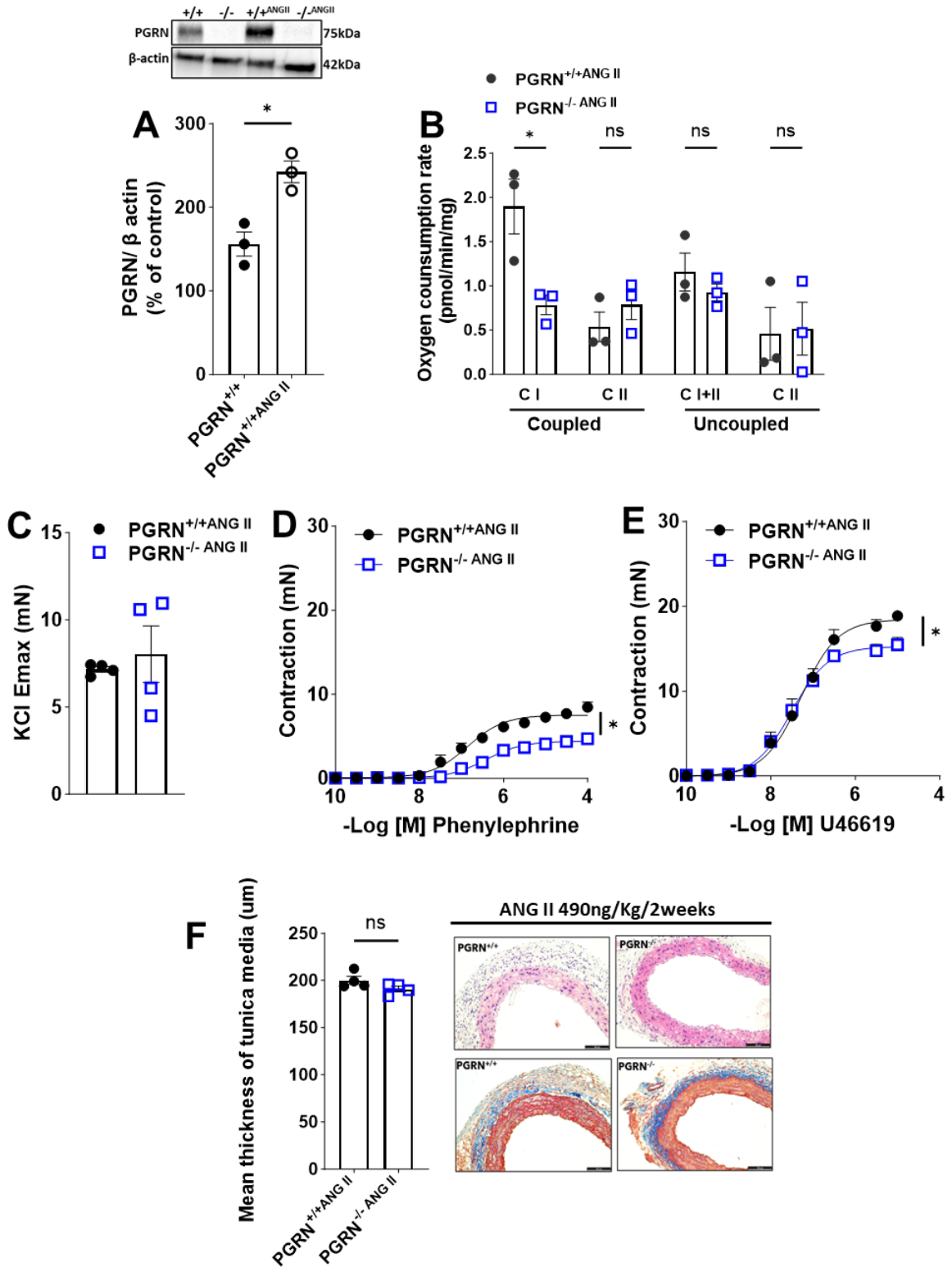

Figure 18. PGRN Deficient Mice Fail to Respond to Angiotensin II-Induced Vascular Hypercontractility

(A) Western blot for PGRN expression in aortae from PGRN+/+ and PGRN-/- mice treated with Angiotensin II (490ng/Kg/day for 14 days, via osmotic mini-pump). β-actin was used as load control. (B) Mitochondrial oxygen consumption rates (OCR) measured using the Oroboros O2k respirometry in fresh aortae of PGRN+/+ and PGRN-/- mice treated with Angiotensin II. (C-E) *Ex vivo* wire myography showing concentration-effect curves to KCl (120mM) (C), phenylephrine (D), and thromboxane A2 analogue (U46619) (E) in endothelium-denuded aortic rings of aortae PGRN+/+ and PGRN-/- mice treated with Angiotensin II. (F) Images of Hematoxylin & eosin and Masson's trichrome stains in aortae from PGRN+/+ and PGRN-/- mice treated with Angiotensin II. Scale bar, 100 μm. Morphometric analysis of media area in PGRN-/- and PGRN+/+ mice aged 12-14 weeks. Data are presented as mean ± SEM (n =3-4). *P < 0.05 vs PGRN-/-

3.0 Discussion

Loss of vascular contraction is a critical factor in CVD pathogenesis limiting the normal function of the artery and increasing the risk of organ damage because of impaired blood flow[178]. However, the mechanisms involved in this phenotype are not well understood. In this study, we uncover a novel and major role for PGRN, which consists in maintaining the VSMC contractility via adjusting mitochondrial quality and dependent on lysosome biogenesis, mitophagy, and complex I biogenesis pathways.

PGRN loss-of-function mutations cause neuronal ceroid lipofuscinosis and FTD-GRN in a dosage-dependent way[42]. PGRN regulates development, survival, function, and maintenance of mammalian cells including vascular cells (VSMC[140] and endothelial cells[139]). Recently, Gerrits et al[179] identified that the neurovascular unit is severely affected in FTD-GRN, while our group described that deficiency in PGRN disturbs endothelial biology and blood pressure regulation [139]. In VSMC, PGRN exerts antimigratory effects via modulating IL-8 formation in atherosclerotic environment[140] and its full-length (~70kDa) acts inhibiting the calcification in calcific aortic valve disease[141]. Therefore, PGRN plays a major role in regulating vascular biology and it seems to be a key protein keeping a contractile VSMC phenotype. Herein, for the first time, we are describing that deficiency in PGRN strikingly affects the contraction of VSMC likely suppressing the amount of contractile proteins and fibrosis and without affecting the vascular structure, at least at 12-16-weeks old mice.

In neuronal[174] and renal cells[63] and in *C. elegans[180]* PGRN acts as a regulator of mitochondrial function via preserving mitochondrial dynamics, biogenesis, and mitochondrial recycling. Mitochondrial dysfunction is part of premature ageing and contributes to appearance of

inflammation, mitochondria-associated oxidative stress, cell senescence, and apoptosis, which are leading causes of CVD[172, 181, 182] including atherosclerosis and aneurysm [96, 183, 184]. From a mechanistic perspective, our observations revealed that the deficiency of PGRN had a multifaceted impact on mitochondrial quality within VSMCs. Notably, VSMCs deficient in PGRN exhibited markers of mitochondrial fragmentation and a decrease in the expression of complex I genes and mass. These alterations subsequently exerted a profound influence on mitochondrial respiration, as evidenced by a reduction in complex I activity, a disrupted NAD+/NADH ratio, and diminished ATP levels. The compromised mitochondrial function culminated in an excessive generation of mtROS. Remarkably, the loss of mitochondrial complex I mass, or activity emerged as a pivotal contributor to redox imbalance and the pathogenesis of cardiovascular disease[185]. Herein, we observed the disruption of PGRN signaling triggered an mtROS overproduction and increased the sensitivity to antimycin A-induced mtROS formation. Notably, PGRN overexpression in VSMC generated high-capacity mitochondria with markers of mitochondria fusion, higher complex I activity, and elevated NAD+/NADH ratio, ATP levels, and antioxidant property (blockage against mtROS formation) followed by restored VSMC hypercontractility. From a therapeutic perspective, we can suggest that overexpressing PGRN in VSMC might regulate mitochondrial capacity and confer protection against CVD via by finely modulating mtROS signaling, fostering mitochondrial complex I biogenesis and enhancing its function. Although we did not investigate by which mechanisms PGRN regulates mitochondrial complex I activity and biogenesis, in neuroblastoma cell line PPARγ activation rescues mitochondrial function from inhibition of complex I, therefore, the suppression of PPARγ in aortae from male and female PGRN deficient mice might be an indicative of impaired complex I related gene expression [177].

Mitochondria are highly dynamic organelles undergoing synchronized cycles of fission and fusion, named mitochondrial dynamics. Such event occurs to maintain mitochondrial shape, distribution, and size[172, 186]. In a positive loop, excess of ROS leads to mitochondrial fission[187], while mitochondria can undergo rapid fragmentation with a concomitant increase in ROS formation[188], therefore in the vasculature PGRN may exert antioxidant property by regulating complex I activity and mitochondria dynamic, as observed before in non-vascular cells[174].

Deficiency in PGRN regulates the expression of PGC1α in non-vascular tissues[63, 189], in line with this observation, we noted a significant decrease in PGC1α in VSMC deficient for PGRN. Surprisingly, this suppression did not result in a reduction of mtDNA. PGC1α is transcriptional coactivator that not only governs mitochondrial biogenesis, but also is linked to antioxidant defense and anti-inflammatory property in endothelial cells and VSMC[175, 176, 190]. Hence, the reduction in PGC1α may affect inflammatory responses and redox balance rather than mitochondrial biogenesis in PGRN-/- VSMC, and perhaps other mitochondrial regulator might be overcoming the impaired PGC1α, including PGC-1β, which shares similar molecular structure and function with PGC-1α[191]. Further research is necessary to explore the interface between PGRN and both PGC1α and β in cardiovascular biology.

PGRN may exert its biological effects as a secreted form, as we have demonstrated before in endothelial cells[139]. Thus, we reconstituted the circulating PGRN levels in PGRN deficient mice (via osmotic mini-pump delivery) or in isolated VSMC. We observed that circulating PGRN does not affect mitochondrial function in fresh aortae, nor in cells treated with rPGRN, suggesting that PGRN is not maintaining the vascular contractility and mitochondrial quality via autocrine or paracrine mechanisms, but perhaps as an intracellular molecule. Thus, we reconstituted the PGRN

levels in fresh aorta via LV delivery to analyze mitochondria respiration and vascular contractility. Returning PGRN in fresh aortae from PGRN deficient mice rescued the mitochondria capacity, mainly via complex I activity, and vascular contractility. This piece of data indicates that intracellular, but not circulating PGRN, regulates the vascular contractility and complex I activity.

Mammalian cells have evolved fine-tuned mechanisms of quality control that help to preserve the functional mitochondria to meet the demand of the cell[192]. Mitophagy is one of the selective autophagy processes to remove accumulated damaged or dysfunctional mitochondria from cells to maintain mitochondrial homeostasis[192]. In diabetic nephropathy, PGRN is crucial regulating renal integrity by regulating mitophagy[63]. In VSMC we observed that PGRN deficiency induces markers of impaired mitophagy flux (accumulation of p62, LC3I/II, PINK, and PARKIN), while overexpressing PGRN in fresh aortae from mt-Keima mice or in VSMC leads to an accelerated mitophagy process. To analyze whether reaccelerating autophagy might be a therapeutic approach to individuals with deficiency in PGRN, we treated mice with spermidine, a natural polyamine with autophagic characteristics [158]and that can extend life span in mammalian organisms [158, 183, 193]. Spermidine induced autophagy, improved the mitochondria function, and rescued the vascular function in PGRN deficient mice, these data suggest that restoration of mitophagy flux is an attractive pharmacological approach to attenuate the cardiovascular risk in patients with loss-of-function of PGRN.

PGRN is a guardian of lysosome biology [106] by regulating lysosome biogenesis in a TFEB dependent manner[194] and lysosome function. Lack of PGRN triggers accumulation of p62 (marker of damaged lysosome[195]) and LAMP1/2[196, 197]. In line with previous findings, PGRN deficient VSMC demonstrated accumulation of p62 and LC3I/II, increased LAMP content, and greater nuclear TFEB levels, although there is more TFEB in the nuclear fraction - an

indicative of higher activity - the autophagic flux is interrupted (increased p62 and LC3II/I accumulation), indicating that TFEB is more active, but the formed lysosomes are imperfect. Such higher TFEB activation might be occurring in an attempt to generate appropriate lysosome and subsequently an adequate autophagy flux, but in an inefficient pathway. Interestingly, high amount of PGRN promoted more TFEB translocation into the nuclei and led to a prominent p62 reduction and increased LC3I/II, which indicates that PGRN induces lysosome TFEB activation and autophagy flux. Thus, complex I activity and biogenesis and disturbed mitophagy are key downstream pathways to PGRN.

Since lack of vascular PGRN is a cardiovascular risk, we challenged mice with Angiotensin II for two distinct reasons. 1. to analyze whether ablation of PGRN would aggravate Angiotensin II-induced mitochondria dysfunction and 2. to examine whether Angiotensin II could restore the vascular contractility in PGRN deficient mice. Normally, Angiotensin II treatment induces vascular hypercontractility[198], upregulates contractile proteins[199], and triggers mitochondria dysfunction[200]. At least with Angiotensin II treatment, lack of PGRN did not affect mitochondrial function, but it blunted the vascular hypercontractility, the vascular PGRN pathway is essential to maintaining the vascular tone and induce vascular contraction.

In this work, we suggest that PGRN pathway is critical regulating the vascular tone by modulating mitochondrial quality by two chronological and distinct mechanisms. PGRN regulates mitochondrial complex I biogenesis and activity and orchestrates mitochondria recycling via maintaining lysosome quality. Subsequently, it preserves vascular bioenergetic pathway and redox balance inhibiting an exacerbated mtROS formation, which conserves the vascular tone. Future research endeavors should delve into the long-term consequences of PGRN deficiency in the context of cardiovascular diseases. Longitudinal studies are needed to assess how PGRN levels

correlate with disease severity and progression in human patients. Finally, our study opens new opportunities not only to cardiovascular biology, but also to examine this pathway in neurodegenerative diseases associated with PGRN mutations, which have been recently associated with perturbation of neurovascular compartment[179], as well.

4.0 List of Tables

Table 1. Sequences of Forward and Reverse Primers Used for RT-PCR

Gene	Primer	Sequence
GAPDH	Forward	GAGAGGCCCTATCCCAACTC
	Reverse	TCAAGAGAGTAGGGAGGGCT
αSMA	Forward	TGCTGACAGAGGCACCACTGAA
	Reverse	CAGTTGTACGTCCAGAGGCATAG
PPARγ	Forward	AGCCTGCGAAAGCCTTTTGGTG
	Reverse	GGCTTCACATTCAGCAAACCTGG
NDUFV2	Forward	ACTCTGACAGCATACTGGAGGC
	Reverse	ACCATTGGTGCGTTCACACAGG
NDUFS8	Forward	TAATACGACTCACTATAGGG
	Reverse	TAGAAGGCACAGTCGAGG
NDUFS4	Forward	TGACAGGCGATACATCCATAT
	Reverse	GAAGTTCTCACAATCACCAGAT
NDUFV1	Forward	TGTGTGAGACGGTGCTGATGGA
	Reverse	CGATGGCTTTCACGATGTCCGT
NDUFAB1	Forward	CATTTGTGCCGCCAGTACAGTG
	Reverse	GGTCCAAACTGTCTAAGCCCAG
NDUFS1	Forward	GTGGATGCTGAAGCCTTAGTAGC
	Reverse	GGAACGTAAGTCTGTACCAGCTC
NDUFB5	Forward	AGGCTATGTCCCAGAACACTGG
	Reverse	CAGCTTCAATCTGAAGGACGGC
ICAM	Forward	AGCGGCTGACGTGTGCAGTAAT
	Reverse	TCTGAGACCTCTGGCTTCGTCA
VCAM	Forward	GATTCTGTGCCCACAGTAAGGC
	Reverse	TGGTCACAGAGCCACCTTCTTG
IL1β	Forward	CCACAGACCTTCCAGGAGAATG
	Reverse	GTGCAGTTCAGTGATCGTACAGG
TNFα	Forward	CTCTTCTGCCTGCTGCACTTTG
	Reverse	ATGGGCTACAGGCTTGTCACTC
IL6	Forward	AGACAGCCACTCACCTCTTCAG
	Reverse	TTCTGCCAGTGCCTCTTTGCTG

Table 2. List of Antibodies

Antibody	Catalog number	Company	Concentration
α-Smooth Muscle Actin	#19245	Cell signaling	1:1000
Total OXPHOS	#ab110413	Abcam	1:500
PERK	#C33E10	Cell signaling	1:1000
PGC-1α	#ab176328	Abcam	1:1000
PINK-1	#ab23707	Abcam	1:1000
Parkin (Prk8)	#ab77924	Abcam	1:1000
DRP1	#5391	Cell signaling	1:1000
Mitofusion-2 (MTF2	#9482	Cell signaling	1:1000
Progranulin	#ab187070	Abcam	1:1000
Progranulin	#AF2557	R&D	1:1000
LC3A/B	#4108	Cell signaling	1:1000
P62	#ab91526	Abcam	1:1000
LAMP	#9091	Cell signaling	1:1000
TFEB	#37681	Cell signaling	1:1000
GAPDH	#8884	Cell signaling	1:1000
β-ACTIN	#A3854	Sigma	1:20000
HISTONE 3	#9715	Cell signaling	1:1000

Bibliography

1. Roth, G.A., et al., Global Burden of Cardiovascular Diseases and Risk Factors, 1990-2019: Update From the GBD 2019 Study. J Am Coll Cardiol, 2020. **76**(25): p. 2982-3021.

2. Tsao, C.W., et al., Heart Disease and Stroke Statistics-2023 Update: A Report From the American Heart Association. Circulation, 2023. **147**(8): p. e93-e621.

3. Brozovich, F.V., et al., Mechanisms of Vascular Smooth Muscle Contraction and the Basis for Pharmacologic Treatment of Smooth Muscle Disorders. Pharmacol Rev, 2016. **68**(2): p. 476-532.

4. Jaminon, A., et al., The Role of Vascular Smooth Muscle Cells in Arterial Remodeling: Focus on Calcification-Related Processes. Int J Mol Sci, 2019. **20**(22).

5. Cao, G., et al., How vascular smooth muscle cell phenotype switching contributes to vascular disease. Cell Commun Signal, 2022. **20**(1): p. 180.

6. Lacolley, P., et al., The vascular smooth muscle cell in arterial pathology: a cell that can take on multiple roles. Cardiovascular Research, 2012. **95**(2): p. 194-204.

7. Chakraborty, R., et al., Targeting smooth muscle cell phenotypic switching in vascular disease. JVS Vasc Sci, 2021. **2**: p. 79-94.

8. Bateman, A., et al., Granulins, a novel class of peptide from leukocytes. Biochem Biophys Res Commun, 1990. **173**(3): p. 1161-8.

9. Bhandari, V., R.G. Palfree, and A. Bateman, Isolation and sequence of the granulin precursor cDNA from human bone marrow reveals tandem cysteine-rich granulin domains. Proc Natl Acad Sci U S A, 1992. **89**(5): p. 1715-9.

10. Zhu, J., et al., Conversion of proepithelin to epithelins: roles of SLPI and elastase in host defense and wound repair. Cell, 2002. **111**(6): p. 867-78.

11. Bateman, A. and H.P. Bennett, Granulins: the structure and function of an emerging family of growth factors. J Endocrinol, 1998. **158**(2): p. 145-51.

12. Brünger, A.T., et al., Crystallography & NMR system: A new software suite for macromolecular structure determination. Acta Crystallogr D Biol Crystallogr, 1998. **54**(Pt 5): p. 905-21.

13. Chitramuthu, B.P., et al., Progranulin modulates zebrafish motoneuron development in vivoand rescues truncation defects associated with knockdown of Survival motor neuron 1. Molecular Neurodegeneration, 2010. **5**(1): p. 41.

14. Hsu, T.Y., V.J. Butler, and A.W. Kao, The Use of Caenorhabditis elegans to Study Progranulin in the Regulation of Programmed Cell Death and Stress Response. Methods Mol Biol, 2018. **1806**: p. 193-206.

15. Tolkatchev, D., et al., Structure dissection of human progranulin identifies well-folded granulin/epithelin modules with unique functional activities. Protein Sci, 2008. **17**(4): p. 711-24.

16. Bateman, A. and H.P. Bennett, The granulin gene family: from cancer to dementia. Bioessays, 2009. **31**(11): p. 1245-54.

17. Ghag, G., et al., Disulfide bonds and disorder in granulin-3: An unusual handshake between structural stability and plasticity. Protein Sci, 2017. **26**(9): p. 1759-1772.

18. Xu, D., et al., Novel MMP-9 substrates in cancer cells revealed by a label-free quantitative proteomics approach. Mol Cell Proteomics, 2008. **7**(11): p. 2215-28.

19. Butler, G.S., et al., Pharmacoproteomics of a metalloproteinase hydroxamate inhibitor in breast cancer cells: dynamics of membrane type 1 matrix metalloproteinase-mediated membrane protein shedding. Mol Cell Biol, 2008. **28**(15): p. 4896-914.

20. Bai, X.H., et al., ADAMTS-7, a direct target of PTHrP, adversely regulates endochondral bone growth by associating with and inactivating GEP growth factor. Mol Cell Biol, 2009. **29**(15): p. 4201-19.

21. Lee, C.W., et al., The lysosomal protein cathepsin L is a progranulin protease. Molecular Neurodegeneration, 2017. **12**(1): p. 55.

22. Kessenbrock, K., et al., Proteinase 3 and neutrophil elastase enhance inflammation in mice by inactivating antiinflammatory progranulin. J Clin Invest, 2008. **118**(7): p. 2438-47.

23. Salazar, D.A., et al., The Progranulin Cleavage Products, Granulins, Exacerbate TDP-43 Toxicity and Increase TDP-43 Levels. J Neurosci, 2015. **35**(25): p. 9315-28.

24. van Wetering, S., et al., Regulation of SLPI and elafin release from bronchial epithelial cells by neutrophil defensins. Am J Physiol Lung Cell Mol Physiol, 2000. **278**(1): p. L51-8.

25. Samejima, T., et al., Secretory leukocyte protease inhibitor and progranulin as possible regulators of cervical remodeling in pregnancy. Journal of Reproductive Immunology, 2021. **143**: p. 103241.

26. Xu, K., et al., Cartilage oligomeric matrix protein associates with granulin-epithelin precursor (GEP) and potentiates GEP-stimulated chondrocyte proliferation. J Biol Chem, 2007. **282**(15): p. 11347-55.

27. Baba, T., et al., Acrogranin, an acrosomal cysteine-rich glycoprotein, is the precursor of the growth-modulating peptides, granulins, and epithelins, and is expressed in somatic as well as male germ cells. Mol Reprod Dev, 1993. **34**(3): p. 233-43.

28. Daniel, R., et al., Cellular Localization of Gene Expression for Progranulin. Journal of Histochemistry & Cytochemistry, 2000. **48**(7): p. 999-1009.

29. Gao, C., et al., Microglia in neurodegenerative diseases: mechanism and potential therapeutic targets. Signal Transduction and Targeted Therapy, 2023. **8**(1): p. 359.

30. Keren-Shaul, H., et al., A Unique Microglia Type Associated with Restricting Development of Alzheimer's Disease. Cell, 2017. **169**(7): p. 1276-1290.e17.

31. Devireddy, S. and S.M. Ferguson, Efficient progranulin exit from the ER requires its interaction with prosaposin, a Surf4 cargo. J Cell Biol, 2022. **221**(2).

32. Shankaran, S.S., et al., Missense mutations in the progranulin gene linked to frontotemporal lobar degeneration with ubiquitin-immunoreactive inclusions reduce progranulin production and secretion. J Biol Chem, 2008. **283**(3): p. 1744-1753.

33. Kleinberger, G., et al., Reduced secretion and altered proteolytic processing caused by missense mutations in progranulin. Neurobiol Aging, 2016. **39**: p. 220.e17-26.

34. Neill, T., et al., EphA2 is a functional receptor for the growth factor progranulin. J Cell Biol, 2016. **215**(5): p. 687-703.

35. Altmann, C., et al., Progranulin promotes peripheral nerve regeneration and reinnervation: role of notch signaling. Mol Neurodegener, 2016. **11**(1): p. 69.

36. Tang, W., et al., The growth factor progranulin binds to TNF receptors and is therapeutic against inflammatory arthritis in mice. Science, 2011. **332**(6028): p. 478-84.

37. Townley, R.A., B.F. Boeve, and E.E. Benarroch, Progranulin: Functions and neurologic correlations. Neurology, 2018. **90**(3): p. 118-125.

38. Hoque, M., M.B. Mathews, and T. Pe'ery, Progranulin (granulin/epithelin precursor) and its constituent granulin repeats repress transcription from cellular promoters. J Cell Physiol, 2010. **223**(1): p. 224-33.

39. Palfree, R.G., H.P. Bennett, and A. Bateman, The Evolution of the Secreted Regulatory Protein Progranulin. PLoS One, 2015. **10**(8): p. e0133749.

40. Wei, F., et al., Induction of PGRN by influenza virus inhibits the antiviral immune responses through downregulation of type I interferons signaling. PLoS Pathog, 2019. **15**(10): p. e1008062.

41. Yan, W., et al., Progranulin Controls Sepsis via C/EBPα-Regulated Il10 Transcription and Ubiquitin Ligase/Proteasome-Mediated Protein Degradation. The Journal of Immunology, 2016. **197**(8): p. 3393-3405.

42. Rhinn, H., et al., Progranulin as a therapeutic target in neurodegenerative diseases. Trends Pharmacol Sci, 2022. **43**(8): p. 641-652.

43. Lomen-Hoerth, C., T. Anderson, and B. Miller, The overlap of amyotrophic lateral sclerosis and frontotemporal dementia. Neurology, 2002. **59**(7): p. 1077-9.

44. Rademakers, R., M. Neumann, and I.R. Mackenzie, Advances in understanding the molecular basis of frontotemporal dementia. Nat Rev Neurol, 2012. **8**(8): p. 423-34.

45. Barohn, R.J., D.C. Dowd, and K.S. Kagan-Hallet, Congenital ceroid-lipofuscinosis. Pediatric neurology, 1992. **8**(1): p. 54-59.

46. Ward, M.E., et al., Individuals with progranulin haploinsufficiency exhibit features of neuronal ceroid lipofuscinosis. Sci Transl Med, 2017. **9**(385).

47. Finger, E.C., Frontotemporal Dementias. Continuum (Minneap Minn), 2016. **22**(2 Dementia): p. 464-89.

48. He, Z., et al., Progranulin is a mediator of the wound response. Nat Med, 2003. **9**(2): p. 225-9.

49. Zhao, Y.P., et al., The promotion of bone healing by progranulin, a downstream molecule of BMP-2, through interacting with TNF/TNFR signaling. Biomaterials, 2013. **34**(27): p. 6412-21.

50. Yin, F., et al., Exaggerated inflammation, impaired host defense, and neuropathology in progranulin-deficient mice. J Exp Med, 2010. **207**(1): p. 117-28.

51. Tao, J., et al., Neuroprotective effects of progranulin in ischemic mice. Brain Res, 2012. **1436**: p. 130-6.

52. Wang, S., et al., Progranulin Is Positively Associated with Intervertebral Disc Degeneration by Interaction with IL-10 and IL-17 Through TNF Pathways. Inflammation, 2018. **41**(5): p. 1852-1863.

53. Chen, J., et al., Serum progranulin irrelated with Breg cell levels, but elevated in RA patients, reflecting high disease activity. Rheumatol Int, 2016. **36**(3): p. 359-64.

54. Keffer, J., et al., Transgenic mice expressing human tumour necrosis factor: a predictive genetic model of arthritis. Embo j, 1991. **10**(13): p. 4025-31.

55. Song, Z., et al., Progranulin Plays a Central Role in Host Defense during Sepsis by Promoting Macrophage Recruitment. Am J Respir Crit Care Med, 2016. **194**(10): p. 1219-1232.

56. Li, M., et al., Progranulin is required for proper ER stress response and inhibits ER stress-mediated apoptosis through TNFR2. Cellular Signalling, 2014. **26**(7): p. 1539-1548.

57. Yu, Y., et al., Progranulin deficiency leads to severe inflammation, lung injury and cell death in a mouse model of endotoxic shock. J Cell Mol Med, 2016. **20**(3): p. 506-17.

58. Tian, G., et al., Recent advances in the study of progranulin and its role in sepsis. International Immunopharmacology, 2020. **79**: p. 106090.

59. Menzel, L., et al., Progranulin protects against exaggerated axonal injury and astrogliosis following traumatic brain injury. Glia, 2017. **65**(2): p. 278-292.

60. Zhou, M., et al., Progranulin protects against renal ischemia/reperfusion injury in mice. Kidney Int, 2015. **87**(5): p. 918-29.

61. Murakoshi, M., et al., Progranulin and Its Receptor Predict Kidney Function Decline in Patients With Type 2 Diabetes. Front Endocrinol (Lausanne), 2022. **13**: p. 849457.

62. Tadagavadi, R.K. and W.B. Reeves, NODding off in acute kidney injury with progranulin? Kidney Int, 2015. **87**(5): p. 873-5.

63. Zhou, D., et al., PGRN acts as a novel regulator of mitochondrial homeostasis by facilitating mitophagy and mitochondrial biogenesis to prevent podocyte injury in diabetic nephropathy. Cell Death Dis, 2019. **10**(7): p. 524.

64. Matsubara, T., et al., PGRN is a key adipokine mediating high fat diet-induced insulin resistance and obesity through IL-6 in adipose tissue. Cell Metab, 2012. **15**(1): p. 38-50.

65. Qu, H., H. Deng, and Z. Hu, Plasma progranulin concentrations are increased in patients with type 2 diabetes and obesity and correlated with insulin resistance. Mediators Inflamm, 2013. **2013**: p. 360190.

66. Yoo, H.J., et al., Implication of progranulin and C1q/TNF-related protein-3 (CTRP3) on inflammation and atherosclerosis in subjects with or without metabolic syndrome. PLoS One, 2013. **8**(2): p. e55744.

67. Li, H., et al., Circulating PGRN Is Significantly Associated With Systemic Insulin Sensitivity and Autophagic Activity in Metabolic Syndrome. Endocrinology, 2014. **155**(9): p. 3493-3507.

68. Hossein-Nezhad, A., et al., Obesity, inflammation and resting energy expenditure: possible mechanism of progranulin in this pathway. Minerva Endocrinol, 2012. **37**(3): p. 255-66.

69. Ahmed, Z., et al., Progranulin in frontotemporal lobar degeneration and neuroinflammation. Journal of Neuroinflammation, 2007. **4**(1): p. 7.

70. Osellame, L.D., T.S. Blacker, and M.R. Duchen, Cellular and molecular mechanisms of mitochondrial function. Best Pract Res Clin Endocrinol Metab, 2012. **26**(6): p. 711-23.

71. Griparic, L. and A.M. van der Bliek, The many shapes of mitochondrial membranes. Traffic, 2001. **2**(4): p. 235-44.

72. Structure and Morphology, in Mitochondria. 1999. p. 15-47.

73. Kirichok, Y., G. Krapivinsky, and D.E. Clapham, The mitochondrial calcium uniporter is a highly selective ion channel. Nature, 2004. **427**(6972): p. 360-364.

74. Zoratti, M., et al., Novel channels of the inner mitochondrial membrane. Biochimica et Biophysica Acta (BBA) - Bioenergetics, 2009. **1787**(5): p. 351-363.

75. Walther, D.M. and D. Rapaport, Biogenesis of mitochondrial outer membrane proteins. Biochim Biophys Acta, 2009. **1793**(1): p. 42-51.

76. Zahedi, R.P., et al., Proteomic Analysis of the Yeast Mitochondrial Outer Membrane Reveals Accumulation of a Subclass of Preproteins. Molecular Biology of the Cell, 2006. **17**(3): p. 1436-1450.

77. Blackstone, N.W., The Quarterly Review of Biology, 2007. **82**(1): p. 44-44.

78. Xie, N., et al., NAD+ metabolism: pathophysiologic mechanisms and therapeutic potential. Signal Transduction and Targeted Therapy, 2020. **5**(1): p. 227.

79. Zorova, L.D., et al., Mitochondrial membrane potential. Anal Biochem, 2018. **552**: p. 50-59.

80. Uittenbogaard, M. and A. Chiaramello, Mitochondrial biogenesis: a therapeutic target for neurodevelopmental disorders and neurodegenerative diseases. Curr Pharm Des, 2014. **20**(35): p. 5574-93.

81. Mishra, P. and D.C. Chan, Mitochondrial dynamics and inheritance during cell division, development and disease. Nat Rev Mol Cell Biol, 2014. **15**(10): p. 634-46.

82. Tyrrell, D.J., et al., Age-Associated Mitochondrial Dysfunction Accelerates Atherogenesis. Circulation Research, 2020. **126**(3): p. 298-314.

83. Angajala, A., et al., Diverse Roles of Mitochondria in Immune Responses: Novel Insights Into Immuno-Metabolism. Front Immunol, 2018. **9**: p. 1605.

84. Wallace, D.C., Mitochondria and cancer. Nature Reviews Cancer, 2012. **12**(10): p. 685-698.

85. Beal, M.F., Mitochondria and neurodegeneration. Novartis Found Symp, 2007. **287**: p. 183-92; discussion 192-6.

86. Chen, Y.-R. and J.L. Zweier, Cardiac Mitochondria and Reactive Oxygen Species Generation. Circulation Research, 2014. **114**(3): p. 524-537.

87. Nakatogawa, H., et al., Dynamics and diversity in autophagy mechanisms: lessons from yeast. Nat Rev Mol Cell Biol, 2009. **10**(7): p. 458-67.

88. Xie, Z. and D.J. Klionsky, Autophagosome formation: core machinery and adaptations. Nat Cell Biol, 2007. **9**(10): p. 1102-9.

89. Aerts, L., et al., PINK1 kinase catalytic activity is regulated by phosphorylation on serines 228 and 402. J Biol Chem, 2015. **290**(5): p. 2798-811.

90. Aguileta, M.A., et al., The E3 ubiquitin ligase parkin is recruited to the 26 S proteasome via the proteasomal ubiquitin receptor Rpn13. J Biol Chem, 2015. **290**(12): p. 7492-505.

91. Ge, P., V.L. Dawson, and T.M. Dawson, PINK1 and Parkin mitochondrial quality control: a source of regional vulnerability in Parkinson's disease. Molecular Neurodegeneration, 2020. **15**(1): p. 20.

92. Tchalla, A.E., et al., Circulating vascular cell adhesion molecule-1 is associated with cerebral blood flow dysregulation, mobility impairment, and falls in older adults. Hypertension, 2015. **66**(2): p. 340-6.

93. Yu, E., et al., Mitochondrial DNA damage can promote atherosclerosis independently of reactive oxygen species through effects on smooth muscle cells and monocytes and correlates with higher-risk plaques in humans. Circulation, 2013. **128**(7): p. 702-12.

94. Yu, E.P.K., et al., Mitochondrial Respiration Is Reduced in Atherosclerosis, Promoting Necrotic Core Formation and Reducing Relative Fibrous Cap Thickness. Arterioscler Thromb Vasc Biol, 2017. **37**(12): p. 2322-2332.

95. de la Fuente-Alonso, A., et al., Aortic disease in Marfan syndrome is caused by overactivation of sGC-PRKG signaling by NO. Nature Communications, 2021. **12**(1): p. 2628.

96. Oller, J., et al., Extracellular Tuning of Mitochondrial Respiration Leads to Aortic Aneurysm. Circulation, 2021. **143**(21): p. 2091-2109.

97. Oller, J., et al., Rewiring Vascular Metabolism Prevents Sudden Death due to Aortic Ruptures-Brief Report. Arterioscler Thromb Vasc Biol, 2022. **42**(4): p. 462-469.

98. Yu, E., K. Foote, and M. Bennett, Mitochondrial function in thoracic aortic aneurysms. Cardiovasc Res, 2018. **114**(13): p. 1696-1698.

99. Swiader, A., et al., Mitophagy acts as a safeguard mechanism against human vascular smooth muscle cell apoptosis induced by atherogenic lipids. Oncotarget, 2016. **7**(20): p. 28821-35.

100. Tang, Y., et al., Compromised mitochondrial remodeling in compensatory hypertrophied myocardium of spontaneously hypertensive rat. Cardiovasc Pathol, 2014. **23**(2): p. 101-6.

101. Dedert, C., et al., Progranulin Preserves Autophagy Flux and Mitochondrial Function in Rat Cortical Neurons Under High Glucose Stress. Front Cell Neurosci, 2022. **16**: p. 874258.

102. De Duve, C. and R. Wattiaux, Functions of lysosomes. Annu Rev Physiol, 1966. **28**: p. 435-92.

103. Finch, N., et al., TMEM106B regulates progranulin levels and the penetrance of FTLD in GRN mutation carriers. Neurology, 2011. **76**(5): p. 467-74.

104. Paushter, D.H., et al., The lysosomal function of progranulin, a guardian against neurodegeneration. Acta Neuropathol, 2018. **136**(1): p. 1-17.

105. Neumann, M., et al., Ubiquitinated TDP-43 in frontotemporal lobar degeneration and amyotrophic lateral sclerosis. Science, 2006. **314**(5796): p. 130-3.

106. Root, J., et al., Lysosome dysfunction as a cause of neurodegenerative diseases: Lessons from frontotemporal dementia and amyotrophic lateral sclerosis. Neurobiol Dis, 2021. **154**: p. 105360.

107. Butler, V.J., et al., Age- and stress-associated C. elegans granulins impair lysosomal function and induce a compensatory HLH-30/TFEB transcriptional response. PLoS Genet, 2019. **15**(8): p. e1008295.

108. Kleinberger, G., et al., Mechanisms of granulin deficiency: lessons from cellular and animal models. Mol Neurobiol, 2013. **47**(1): p. 337-60.

109. Solchenberger, B., et al., Granulin knock out zebrafish lack frontotemporal lobar degeneration and neuronal ceroid lipofuscinosis pathology. PLoS One, 2015. **10**(3): p. e0118956.

110. Wu, Y., et al., Microglial lysosome dysfunction contributes to white matter pathology and TDP-43 proteinopathy in GRN-associated FTD. Cell Rep, 2021. **36**(8): p. 109581.

111. Feng, T., et al., Loss of TMEM106B and PGRN leads to severe lysosomal abnormalities and neurodegeneration in mice. EMBO Rep, 2020. **21**(10): p. e50219.

112. Gowrishankar, S., et al., Massive accumulation of luminal protease-deficient axonal lysosomes at Alzheimer's disease amyloid plaques. Proc Natl Acad Sci U S A, 2015. **112**(28): p. E3699-708.

113. Zhou, X., et al., Regulation of cathepsin D activity by the FTLD protein progranulin. Acta Neuropathol, 2017. **134**(1): p. 151-153.

114. Butler, V.J., et al., Progranulin Stimulates the In Vitro Maturation of Pro-Cathepsin D at Acidic pH. J Mol Biol, 2019. **431**(5): p. 1038-1047.

115. Tyynelä, J., et al., A mutation in the ovine cathepsin D gene causes a congenital lysosomal storage disease with profound neurodegeneration. Embo j, 2000. **19**(12): p. 2786-92.

116. Beel, S., et al., Progranulin functions as a cathepsin D chaperone to stimulate axonal outgrowth in vivo. Hum Mol Genet, 2017. **26**(15): p. 2850-2863.

117. Valdez, C., et al., Progranulin-mediated deficiency of cathepsin D results in FTD and NCL-like phenotypes in neurons derived from FTD patients. Hum Mol Genet, 2017. **26**(24): p. 4861-4872.

118. Butler, V.J., et al., Multi-Granulin Domain Peptides Bind to Pro-Cathepsin D and Stimulate Its Enzymatic Activity More Effectively Than Progranulin in Vitro. Biochemistry, 2019. **58**(23): p. 2670-2674.

119. Zhou, X., et al., Prosaposin facilitates sortilin-independent lysosomal trafficking of progranulin. J Cell Biol, 2015. **210**(6): p. 991-1002.

120. Jian, J., et al., Association Between Progranulin and Gaucher Disease. EBioMedicine, 2016. **11**: p. 127-137.

121. Simon, M.J., et al., Lysosomal functions of progranulin and implications for treatment of frontotemporal dementia. Trends in Cell Biology, 2023. **33**(4): p. 324-339.

122. Arrant, A.E., et al., Impaired β-glucocerebrosidase activity and processing in frontotemporal dementia due to progranulin mutations. Acta Neuropathologica Communications, 2019. **7**(1): p. 218.

123. Lang, C.M., et al., Membrane orientation and subcellular localization of transmembrane protein 106B (TMEM106B), a major risk factor for frontotemporal lobar degeneration. J Biol Chem, 2012. **287**(23): p. 19355-65.

124. Logan, T., et al., Rescue of a lysosomal storage disorder caused by Grn loss of function with a brain penetrant progranulin biologic. Cell, 2021. **184**(18): p. 4651-4668.e25.

125. Papadopoulos, C., B. Kravic, and H. Meyer, Repair or Lysophagy: Dealing with Damaged Lysosomes. Journal of Molecular Biology, 2020. **432**(1): p. 231-239.

126. Pan, C., et al., The Biofabrication of Diseased Artery In Vitro Models. Micromachines (Basel), 2022. **13**(2).

127. Zhang, W., et al., FAM3B mediates high glucose-induced vascular smooth muscle cell proliferation and migration via inhibition of miR-322-5p. Scientific Reports, 2017. **7**(1): p. 2298.

128. Tang, H.Y., et al., Vascular Smooth Muscle Cells Phenotypic Switching in Cardiovascular Diseases. Cells, 2022. **11**(24).

129. Chen, R., et al., Phenotypic Switching of Vascular Smooth Muscle Cells in Atherosclerosis. Journal of the American Heart Association, 2023. **12**(20): p. e031121.

130. Zhang, D., et al., The Etiology and Molecular Mechanism Underlying Smooth Muscle Phenotype Switching in Intimal Hyperplasia of Vein Graft and the Regulatory Role of microRNAs. Front Cardiovasc Med, 2022. **9**: p. 935054.

131. Hahn, C. and M.A. Schwartz, The Role of Cellular Adaptation to Mechanical Forces in Atherosclerosis. Arteriosclerosis, Thrombosis, and Vascular Biology, 2008. **28**(12): p. 2101-2107.

132. Shi, J., et al., Metabolism of vascular smooth muscle cells in vascular diseases. American Journal of Physiology-Heart and Circulatory Physiology, 2020. **319**(3): p. H613-H631.

133. Zhu, Y., et al., Progranulin deficiency leads to enhanced age-related cardiac hypertrophy through complement C1q-induced β-catenin activation. J Mol Cell Cardiol, 2020. **138**: p. 197-211.

134. Fu, Y., et al., Therapeutic Potential of Progranulin in Hyperhomocysteinemia-Induced Cardiorenal Dysfunction. Hypertension, 2017. **69**(2): p. 259-266.

135. Sasaki, T., et al., Progranulin deficiency exacerbates cardiac remodeling after myocardial infarction. FASEB BioAdvances, 2023. **5**(10): p. 395-411.

136. Sasaki, T., et al., Effects of progranulin on the pathological conditions in experimental myocardial infarction model. Sci Rep, 2020. **10**(1): p. 11842.

137. Kawase, R., et al., Deletion of progranulin exacerbates atherosclerosis in ApoE knockout mice. Cardiovasc Res, 2013. **100**(1): p. 125-33.

138. Hwang, H.J., et al., Progranulin protects vascular endothelium against atherosclerotic inflammatory reaction via Akt/eNOS and nuclear factor-κB pathways. PLoS One, 2013. **8**(9): p. e76679.

139. Bruder-Nascimento, A., et al., Progranulin Maintains Blood Pressure and Vascular Tone Dependent on EphrinA2 and Sortilin1 Receptors and Endothelial Nitric Oxide Synthase Activation. J Am Heart Assoc, 2023. **12**(16): p. e030353.

140. Kojima, Y., et al., Progranulin expression in advanced human atherosclerotic plaque. Atherosclerosis, 2009. **206**(1): p. 102-8.

141. Huang, G., et al., Potential role of full-length and nonfull-length progranulin in affecting aortic valve calcification. J Mol Cell Cardiol, 2020. **141**: p. 93-104.

142. Wessels, A., Cardiovascular Developmental Biology Research² Elucidating Mechanisms Underlying Congenital and Acquired Heart Diseases. J. Cardiovasc. Dev. Dis, 2014. **1**: p. 1-2.

143. Zhang, Y.N., et al., Phenotypic switching of vascular smooth muscle cells in the 'normal region' of aorta from atherosclerosis patients is regulated by miR-145. J Cell Mol Med, 2016. **20**(6): p. 1049-61.

144. Glanz, V.Y., et al., The role of mitochondria in cardiovascular diseases related to atherosclerosis. Front Biosci (Elite Ed), 2020. **12**(1): p. 102-112.

145. Shi, N. and S.Y. Chen, Smooth Muscle Cells Move With Mitochondria. Arterioscler Thromb Vasc Biol, 2018. **38**(6): p. 1255-1257.

146. Qin, H.L., et al., Arterial remodeling: the role of mitochondrial metabolism in vascular smooth muscle cells. Am J Physiol Cell Physiol, 2023. **324**(1): p. C183-c192.

147. Xia, Y., et al., Mitochondrial Homeostasis in VSMCs as a Central Hub in Vascular Remodeling. Int J Mol Sci, 2023. **24**(4).

148. Song, Y., et al., Mitochondrial Quality Control in the Maintenance of Cardiovascular Homeostasis: The Roles and Interregulation of UPS, Mitochondrial Dynamics and Mitophagy. Oxid Med Cell Longev, 2021. **2021**: p. 3960773.

149. Mao, Y., J. Ren, and L. Yang, FUN14 Domain Containing 1 (FUNDC1): A Promising Mitophagy Receptor Regulating Mitochondrial Homeostasis in Cardiovascular Diseases. Front Pharmacol, 2022. **13**: p. 887045.

150. De Muynck, L. and P. Van Damme, Cellular effects of progranulin in health and disease. J Mol Neurosci, 2011. **45**(3): p. 549-60.

151. D'Alton, S. and J. Lewis, Understanding the role of progranulin in Alzheimer's disease. Nature Medicine, 2014. **20**(10): p. 1099-1100.

152. Jian, J., et al., Progranulin: A key player in autoimmune diseases. Cytokine, 2018. **101**: p. 48-55.

153. Belin de Chantemèle, E.J., et al., Impact of leptin-mediated sympatho-activation on cardiovascular function in obese mice. Hypertension, 2011. **58**(2): p. 271-9.

154. Bruder-Nascimento, T., et al., Leptin Restores Endothelial Function via Endothelial PPARγ-Nox1-Mediated Mechanisms in a Mouse Model of Congenital Generalized Lipodystrophy. Hypertension, 2019. **74**(6): p. 1399-1408.

155. Brand, M.D. and D.G. Nicholls, Assessing mitochondrial dysfunction in cells. Biochem J, 2011. **435**(2): p. 297-312.

156. Chinopoulos, C., et al., Measurement of ADP-ATP exchange in relation to mitochondrial transmembrane potential and oxygen consumption. Methods Enzymol, 2014. **542**: p. 333-48.

157. Makrecka-Kuka, M., G. Krumschnabel, and E. Gnaiger, High-Resolution Respirometry for Simultaneous Measurement of Oxygen and Hydrogen Peroxide Fluxes in Permeabilized Cells, Tissue Homogenate and Isolated Mitochondria. Biomolecules, 2015. **5**(3): p. 1319-38.

158. Eisenberg, T., et al., Cardioprotection and lifespan extension by the natural polyamine spermidine. Nat Med, 2016. **22**(12): p. 1428-1438.

159. Cau, S.B., et al., Angiotensin-II activates vascular inflammasome and induces vascular damage. Vascul Pharmacol, 2021. **139**: p. 106881.

160. Sibinga, N.E., et al., Collagen VIII is expressed by vascular smooth muscle cells in response to vascular injury. Circ Res, 1997. **80**(4): p. 532-41.

161. Grootaert, M.O., et al., Defective autophagy in vascular smooth muscle cells accelerates senescence and promotes neointima formation and atherogenesis. Autophagy, 2015. **11**(11): p. 2014-2032.

162. Bruder-Nascimento, T., et al., Angiotensin II induces Fat1 expression/activation and vascular smooth muscle cell migration via Nox1-dependent reactive oxygen species generation. J Mol Cell Cardiol, 2014. **66**: p. 18-26.

163. Bruder-Nascimento, T., et al., Atorvastatin inhibits pro-inflammatory actions of aldosterone in vascular smooth muscle cells by reducing oxidative stress. Life Sci, 2019. **221**: p. 29-34.

164. Gunther, S., et al., Functional angiotensin II receptors in cultured vascular smooth muscle cells. J Cell Biol, 1982. **92**(2): p. 289-98.

165. Singh, S., et al., CCR5 antagonist treatment inhibits vascular injury by regulating NADPH oxidase 1. Biochem Pharmacol, 2022. **195**: p. 114859.

166. Zhang, Q., et al., Collagen gel contraction assays: From modelling wound healing to quantifying cellular interactions with three-dimensional extracellular matrices. Eur J Cell Biol, 2022. **101**(3): p. 151253.

167. Sakota, Y., et al., Collagen gel contraction assay using human bronchial smooth muscle cells and its application for evaluation of inhibitory effect of formoterol. Biol Pharm Bull, 2014. **37**(6): p. 1014-20.

168. Nadanaciva, S., et al., Assessment of drug-induced mitochondrial dysfunction via altered cellular respiration and acidification measured in a 96-well platform. Journal of Bioenergetics and Biomembranes, 2012. **44**(4): p. 421-437.

169. Myers, M.B., R.A. Mittelstaedt, and R.H. Heflich, Using ΦX174 DNA as an exogenous reference for measuring mitochondrial DNA copy number. BioTechniques, 2009. **47**(4): p. 867-869.

170. Beręsewicz, M., et al., The Effect of a Novel c.820C>T (Arg274Trp) Mutation in the Mitofusin 2 Gene on Fibroblast Metabolism and Clinical Manifestation in a Patient. PLoS One, 2017. **12**(1): p. e0169999.

171. Livak, K.J. and T.D. Schmittgen, Analysis of Relative Gene Expression Data Using Real-Time Quantitative PCR and the 2−ΔΔCT Method. Methods, 2001. **25**(4): p. 402-408.

172. Dromparis, P. and E.D. Michelakis, Mitochondria in vascular health and disease. Annu Rev Physiol, 2013. **75**: p. 95-126.

173. Sun, N., et al., A fluorescence-based imaging method to measure in vitro and in vivo mitophagy using mt-Keima. Nature Protocols, 2017. **12**(8): p. 1576-1587.

174. Rodriguez-Perinan, G., et al., Progranulin Deficiency Induces Mitochondrial Dysfunction in Frontotemporal Lobar Degeneration with TDP-43 Inclusions. Antioxidants (Basel), 2023. **12**(3).

175. Xiong, S., et al., Peroxisome proliferator-activated receptor gamma coactivator-1alpha is a central negative regulator of vascular senescence. Arterioscler Thromb Vasc Biol, 2013. **33**(5): p. 988-98.

176. Kim, H.J., et al., Effects of PGC-1alpha on TNF-alpha-induced MCP-1 and VCAM-1 expression and NF-kappaB activation in human aortic smooth muscle and endothelial cells. Antioxid Redox Signal, 2007. **9**(3): p. 301-7.

177. Corona, J.C., S.C. de Souza, and M.R. Duchen, PPARgamma activation rescues mitochondrial function from inhibition of complex I and loss of PINK1. Exp Neurol, 2014. **253**: p. 16-27.

178. Holmberg, J., et al., Loss of Vascular Myogenic Tone in miR-143/145 Knockout Mice Is Associated With Hypertension-Induced Vascular Lesions in Small Mesenteric Arteries. Arteriosclerosis, Thrombosis, and Vascular Biology, 2018. **38**(2): p. 414-424.

179. Gerrits, E., et al., Neurovascular dysfunction in GRN-associated frontotemporal dementia identified by single-nucleus RNA sequencing of human cerebral cortex. Nat Neurosci, 2022. **25**(8): p. 1034-1048.

180. Doyle, J.J., et al., Chemical and genetic rescue of in vivo progranulin-deficient lysosomal and autophagic defects. Proc Natl Acad Sci U S A, 2021. **118**(25).

181. Siasos, G., et al., Mitochondria and cardiovascular diseases-from pathophysiology to treatment. Ann Transl Med, 2018. **6**(12): p. 256.

182. Yu, E., J. Mercer, and M. Bennett, Mitochondria in vascular disease. Cardiovasc Res, 2012. **95**(2): p. 173-82.

183. Tyrrell, D.J., et al., Age-Associated Mitochondrial Dysfunction Accelerates Atherogenesis. Circ Res, 2020. **126**(3): p. 298-314.

184. Minamino, T. and I. Komuro, Vascular cell senescence: contribution to atherosclerosis. Circ Res, 2007. **100**(1): p. 15-26.

185. Forte, M., et al., Mitochondrial complex I deficiency and cardiovascular diseases: current evidence and future directions. J Mol Med (Berl), 2019. **97**(5): p. 579-591.

186. Chistiakov, D.A., et al., Mitochondrial aging and age-related dysfunction of mitochondria. Biomed Res Int, 2014. **2014**: p. 238463.

187. Chuang, K.C., et al., Imiquimod-induced ROS production disrupts the balance of mitochondrial dynamics and increases mitophagy in skin cancer cells. J Dermatol Sci, 2020. **98**(3): p. 152-162.

188. Yu, T., J.L. Robotham, and Y. Yoon, Increased production of reactive oxygen species in hyperglycemic conditions requires dynamic change of mitochondrial morphology. Proc Natl Acad Sci U S A, 2006. **103**(8): p. 2653-8.

189. Zhou, B., et al., Progranulin induces adipose insulin resistance and autophagic imbalance via TNFR1 in mice. J Mol Endocrinol, 2015. **55**(3): p. 231-43.

190. Kadlec, A.O., et al., Role of PGC-1alpha in Vascular Regulation: Implications for Atherosclerosis. Arterioscler Thromb Vasc Biol, 2016. **36**(8): p. 1467-74.

191. St-Pierre, J., et al., Bioenergetic analysis of peroxisome proliferator-activated receptor gamma coactivators 1alpha and 1beta (PGC-1alpha and PGC-1beta) in muscle cells. J Biol Chem, 2003. **278**(29): p. 26597-603.

192. Patergnani, S., et al., Methods to Monitor Mitophagy and Mitochondrial Quality: Implications in Cancer, Neurodegeneration, and Cardiovascular Diseases. Methods Mol Biol, 2021. **2310**: p. 113-159.

193. Ni, Y.Q. and Y.S. Liu, New Insights into the Roles and Mechanisms of Spermidine in Aging and Age-Related Diseases. Aging Dis, 2021. **12**(8): p. 1948-1963.

194. Tanaka, Y., et al., Increased lysosomal biogenesis in activated microglia and exacerbated neuronal damage after traumatic brain injury in progranulin-deficient mice. Neuroscience, 2013. **250**: p. 8-19.

195. Tan, J.X. and T. Finkel, A phosphoinositide signalling pathway mediates rapid lysosomal repair. Nature, 2022. **609**(7928): p. 815-821.

196. Chang, M.C., et al., Progranulin deficiency causes impairment of autophagy and TDP-43 accumulation. J Exp Med, 2017. **214**(9): p. 2611-2628.

197. Tanaka, Y., et al., Possible involvement of lysosomal dysfunction in pathological changes of the brain in aged progranulin-deficient mice. Acta Neuropathol Commun, 2014. **2**: p. 78.

198. Ryan, M.J., et al., Angiotensin II-induced vascular dysfunction is mediated by the AT1A receptor in mice. Hypertension, 2004. **43**(5): p. 1074-9.

199. Xu, H., et al., VSMC-specific EP4 deletion exacerbates angiotensin II-induced aortic dissection by increasing vascular inflammation and blood pressure. Proc Natl Acad Sci U S A, 2019. **116**(17): p. 8457-8462.

200. Doughan, A.K., D.G. Harrison, and S.I. Dikalov, Molecular mechanisms of angiotensin II-mediated mitochondrial dysfunction: linking mitochondrial oxidative damage and vascular endothelial dysfunction. Circ Res, 2008. **102**(4): p. 488-96.